

1-1-2003

## Topological and synchronicity effects in reaction efficiency

Jonathan Lee Bentz  
*Iowa State University*

Follow this and additional works at: <https://lib.dr.iastate.edu/rtd>

---

### Recommended Citation

Bentz, Jonathan Lee, "Topological and synchronicity effects in reaction efficiency" (2003). *Retrospective Theses and Dissertations*. 19902.  
<https://lib.dr.iastate.edu/rtd/19902>

This Thesis is brought to you for free and open access by the Iowa State University Capstones, Theses and Dissertations at Iowa State University Digital Repository. It has been accepted for inclusion in Retrospective Theses and Dissertations by an authorized administrator of Iowa State University Digital Repository. For more information, please contact [digirep@iastate.edu](mailto:digirep@iastate.edu).

**Topological and synchronicity effects in reaction efficiency**

by

Jonathan Lee Bentz

A thesis submitted to the graduate faculty  
in partial fulfillment of the requirements for the degree of

MASTER OF SCIENCE

Major: Physical Chemistry

Program of Study Committee:  
John J. Kozak, Major Professor  
Jim Evans  
Gerald Small

Iowa State University

Ames, Iowa

2003

Copyright © Jonathan Lee Bentz, 2003. All rights reserved.

Graduate College  
Iowa State University

This is to certify that the master's thesis of  
Jonathan Lee Bentz  
has met the thesis requirements of Iowa State University

Signatures have been redacted for privacy

---

## TABLE OF CONTENTS

<b>LIST OF TABLES</b> . . . . .	v
<b>LIST OF FIGURES</b> . . . . .	vi
<b>CHAPTER 1. General introduction</b> . . . . .	1
1.1 Introduction . . . . .	1
1.2 Thesis organization . . . . .	6
<b>CHAPTER 2. Efficiency of encounter-controlled reaction between diffusing reactants in a finite lattice: topology and boundary effects</b> . . . . .	8
2.1 Introduction . . . . .	9
2.2 Euclidean dimension, $d = 1$ . . . . .	11
2.3 Euclidean dimension, $d = 2$ . . . . .	16
2.4 Higher dimensions and fractal structures . . . . .	20
2.4.1 Euclidean dimension, $d = 3$ . . . . .	20
2.4.2 Fractal dimension, $D = \ln 3 / \ln 2$ . . . . .	20
2.5 Conclusions . . . . .	24
<b>CHAPTER 3. Synchronous vs. asynchronous dynamics of diffusion-controlled reactions</b> . . . . .	27
3.1 Introduction . . . . .	28
3.2 Formulation of the problem: two-walker vs. one-walker picture . . . . .	30
3.3 Connection with ruin problem and analytical solution . . . . .	34
3.4 Monte Carlo results in two and three dimensions . . . . .	42
3.5 Comparison with continuum approximation . . . . .	42

3.6	Conclusions and outlook . . . . .	44
<b>CHAPTER 4.</b>	<b>General conclusions . . . . .</b>	<b>55</b>
4.1	General discussion . . . . .	55
4.2	Future research . . . . .	57
<b>APPENDIX</b>	<b>One Dimensional Example . . . . .</b>	<b>59</b>
<b>REFERENCES</b>	<b>. . . . .</b>	<b>65</b>
<b>ACKNOWLEDGEMENTS</b>	<b>. . . . .</b>	<b>68</b>

## LIST OF TABLES

Table 2.1	Analytic results for Platonic solids and planar analogues with periodic boundary conditions . . . . .	18
Table 2.2	Walklength results for successive Sierpinski generation gaskets. . . . .	23
Table 3.1	Analytic expressions for $\langle n \rangle$ . . . . .	39
Table 3.2	Values of $p_{min}$ with 4-digit accuracy. . . . .	40
Table 3.3	Theoretical vs. simulation value of $\langle n \rangle$ for $N = 7$ . . . . .	41
Table 3.4	Theoretical vs. simulation value of $\langle n \rangle$ for $N = 8$ . . . . .	41

## LIST OF FIGURES

Figure 2.1	Periodic $d = 1$ lattices with a) $N = 3$ and b) $N = 4$ . . . . .	12
Figure 2.2	a) Correspondence between confining and periodic boundary conditions for the two symmetry-distinct trap configurations in a confining 4-site lattice. Sites with same numbers are symmetry-equivalent. b) Four site confining lattice. . . . .	14
Figure 2.3	$\Gamma$ vs. $N$ in $d = 1$ . The curve for the periodic case is generated from the exact analytical results and the data for the confining case is from Monte Carlo simulations. . . . .	15
Figure 2.4	$\langle n \rangle_1$ vs. $\langle n \rangle_2$ in $d = 1$ . The slopes of the best-fit lines are: Periodic = 1.97 and Confining = 2.35. $N_{\min} = 49$ for the periodic case ( $N_{\min}$ is the smallest data point used in the calculation of the best fit curve.) Both curves have R values of greater than 0.999. . . . .	16
Figure 2.5	$\langle n \rangle_1$ vs. $\langle n \rangle_2$ in $d = 2$ . The slopes of the best-fit lines are: Confining = 1.66, Even = 1.25, Odd = 1.42, Cube Surface = 1.47. All data are calculated from simulations. The values of $N_{\min}$ are: Confining = 25, Even = 100, Odd = 81, Cube Surface = 24. All R values are greater than 0.999. . . . .	17
Figure 2.6	$\langle n \rangle_1$ vs. $\langle n \rangle_2$ in $d = 3$ . The slopes of the best-fit lines are: Odd = 1.22, Even = 0.72, Confining = 1.42. All data are calculated from simulations. $N_{\min} = 8$ for all the curves with all R values greater than 0.999. . . . .	21

Figure 2.7	$\Gamma$ vs. $N$ in $d = 3$ subject to confining boundary conditions; all data are calculated from simulations. . . . .	22
Figure 3.1	a) two-walker system on a seven-site periodic lattice (walkers represented by black circles). b) Equivalent one-walker system with trap. For convenience, the walker labels $A$ and $B$ in Fig. 3.1a have been left out. The arrows in Fig. 3.1a indicate that both walkers perform a synchronous step. In Fig. 1b this corresponds to a two-site jump of the walker. . . . .	31
Figure 3.2	Lattice transformation for the one-walker system displayed in Fig. 3.1b.	32
Figure 3.3	Replacement of the traps $T$ at each end site of the transformed lattice by two absorbing sites $r$ . . . . .	33
Figure 3.4	Mean encounter time as a function of the lattice size for the purely synchronous case $\langle n \rangle = \langle n \rangle^{(1)}$ (circles) and the purely asynchronous case $\langle n \rangle = \langle n \rangle^{(0)}$ (crosses). . . . .	37
Figure 3.5	Ratio $\langle n \rangle^{(0)}/\langle n \rangle^{(1)}$ as a function of $N$ . Note that the value of the ratio is the same for two consecutive odd and even values of $N$ . The inset displays the behaviour for small $N$ . . . . .	38
Figure 3.6	$z$ -distribution of the encounter time in the cases $p = 0$ (dashed lines) and $p = 1$ (continuous lines) for a) $N = 3, 5, 7$ and b) $N = 9, 11$ . For $N = 3$ both cases display the same flat distribution. . . . .	47
Figure 3.7	$z$ -distribution of the encounter time for $p = 0$ (dashed lines) and $p = 1$ (continuous lines) for a) $N = 6, 10$ and b) $N = 4, 8$ . . . . .	48
Figure 3.8	Mean encounter time as a function of $p$ for a) $N = 2, \dots, 5$ and b) $N = 6, \dots, 9$ . . . . .	49
Figure 3.9	a) $p$ -dependence of $\langle n \rangle_z$ for all possible values of $d_z$ on a lattice with a) 10 sites b) 9 sites. . . . .	50
Figure 3.10	Mean encounter time as a function of $p$ for two walkers on a $2d$ square planar lattice with periodic boundary conditions. . . . .	51



Figure 3.11	Mean encounter time as a function of $p$ for two walkers on a $3d$ cubic lattice with periodic boundary conditions. . . . .	51
Figure 3.12	Ratio $\langle n \rangle^{(0)} / \langle n \rangle$ as a function of $p$ . . . . .	52
Figure A.1	One dimensional 5-site lattice, with the sites in the circles denoting the lattice sites and the dashed boxes denoting the connectivity of the terminal sites due to the periodicity of the lattice. . . . .	61

## CHAPTER 1. General introduction

### 1.1 Introduction

There are both theoretical and experimental reasons for studying the influence of geometry and boundary conditions on the efficiency of diffusion-reaction processes. First, one would like to isolate effects that are independent of the boundaries of the domain in which the diffusion-reaction processes take place, and for this, periodic boundary conditions are usually imposed. Over the last several years, however, there has been an avalanche of experimental work published on the study of diffusion-reaction processes in micro-heterogeneous media<sup>1</sup> (micelles, clays, zeolites, etc.), with systems of finite extent (nanosystems) showing non-classical behavior (i.e., departures from “mean field” behavior). Therefore, in Chapter 2 we have also examined in tandem with periodic boundary conditions, systems subject to confining boundary conditions. Specifically, in adopting confining boundary conditions, one imposes the condition that if a diffusing particle attempts to exit the lattice from a given boundary site, it is simply reset at that boundary site.

Recently, the modeling of diffusion-controlled reactions on lattices has attracted renewed interest due to synergies with some research areas like e.g. heterogeneous catalysis [2, 3, 4], trapping problems [5], spin models [6], game theory [7], population dynamics [8] or biological problems [9]. An issue common to these systems is the important role played by the coexistence of different intrinsic time scales, the lattice characteristics (size and dimensionality) and many-body effects. The interplay of these ingredients may strongly affect the efficiency with which statistical processes such as front propagation on catalytic substrates, the spread of an infection, kink propagation in magnetic systems, or exciton trapping in photosynthetic cells take place.

---

<sup>1</sup>For a review see ref. [1].

In order to obtain analytical insight for such systems, it is often necessary to make simplifying assumptions which nevertheless preserve their main generic features.

In this spirit, a prototypical diffusion-reaction system consists of two interacting walkers performing nearest neighbor jumps on a lattice [10]. The walkers are assumed to react with each other whenever they meet at the same lattice site or attempt to exchange positions. Each of such “encounters” results in instantaneous reaction, the process therefore being diffusion-controlled. Regardless of the particular outcome of the reaction, a measure for its efficiency will be clearly given by the mean encounter time of both walkers.

In a pioneering work, Montroll investigated a simplified version of the problem in which one of the walkers is stationary, thereby playing the role of a fixed trap [11]. In a recent article [12], Montroll’s results have been extended with the help of a Markovian method to account for the possibility of simultaneous displacement of the walkers. In Chapter 3, the problem is further extended to the case in which the motion of the walkers consists of a random sequence of two different events: at each tick of the clock, a synchronous event takes place with probability  $p$ , i.e., both walkers hop simultaneously to randomly chosen nearest neighbor sites. Alternatively, an asynchronous event takes place with probability  $1 - p$ , i.e. one of the walkers performs a nearest neighbor jump while the other remains immobile. Thus, the parameter  $p$  interpolates between the one walker plus trap case studied by Montroll ( $p = 0$ ) and the case of two simultaneously moving walkers ( $p = 1$ ). A question we shall investigate here concerns the influence of the degree of synchronicity  $p$  of the walkers and the size  $N$  of the lattice in which they are embedded upon the reaction’s efficiency.

Our model may be of interest in several contexts. One can e.g. easily accommodate it to allow for events in which both walkers remain immobile in the original reference frame. Thus, three qualitative different joint events become possible for the two-walker system, which can e.g. be interpreted as resulting from a combination of two internal states for each of the walkers, namely a diffusing and an immobile state. Such two-state random walks [13, 14, 15] are frequently used to model chromatographic [16] or electrophoretic separation processes, in which the propagation of charged particles in an external field may be occasionally stopped by

entanglement with the molecules of the substrate. Such systems, along with hopping models for transport and recombination of carriers in solids [17, 18, 19], might provide additional motivation for considering a generalized version of the random walk.

A different approach suggests to regard the fluctuations in the diffusivity of the walkers as a result of random fluctuations of lattice sites switching between a conducting and a stopping state, whereby the translational invariance of the lattice is preserved on average. An alternative formulation of the problem in terms of fluctuating dichotomous barriers between sites also seems possible [20]. Such models for dynamic random media are relevant for the description of several physiochemical processes like e.g. ligand diffusion in proteins [21] or proton migration in water [22].

On the other hand, if one goes back to the original picture of two dissimilar walkers  $A$  and  $B$ , the model may be regarded as a schematized starting point for describing the dynamics of exciton absorption in biological light-harvesting systems [23]. In photosynthetic cells, a photon is absorbed by the pigment molecules (e.g. chlorophyll) in the cell and may give rise to an excited energy state. The exciton hops by resonant energy transfer through a network or lattice of 200-500 pigment molecules (antenna system) and can be eventually trapped at a reaction center [24], which is usually considered to be immobile within the time scale for trapping (a few hundred picoseconds). The exciton energy is then used to trigger a series of redox processes in the chain of chemical reactions leading to the production of sugars and carbohydrates. Thus, one of the time-limiting steps for the production of oxygen is precisely the absorption of the exciton by the trapping center. If we allow for a certain mobility of the reaction center (thereby generalizing Montroll's approach for exciton trapping), we can identify the latter with a slowly hopping walker, say the  $A$  walker, while the propagating exciton would play the role of the  $B$  walker. As long as the hopping rate of the  $A$  walker remains small, the situation may be identified with the almost purely asynchronous case (small  $p$ ); this is normally the case in *in vivo* light-harvesting systems.

The class of problems we studied can be viewed as Markov processes. (A thorough treat-

ment can be found in refs. [25, 28, 29].) Let

$$P_n(y_1, t_1; y_2, t_2; \dots; y_n, t_n) \quad (1.1)$$

be the probability of the system to be in state  $y_n$  at time  $t_n$  where  $t$  takes on only positive discrete values. Consider the case where  $y_n$  is also a function of a random variable and we know that all the random variables which contribute to each state  $y_n$  are independent of each other. Now let

$$P_{1|n-1}(y_n, t_n | y_{n-1}, t_{n-1}; y_{n-2}, t_{n-2}; \dots; y_1, t_1) \quad (1.2)$$

be the conditional probability that the system in state  $y_{n-1}$  at time  $t_{n-1}$  (and thus all previous states  $y_1, \dots, y_{n-1}$  at times  $t_1, \dots, t_{n-1}$  which are specified in the right hand side of the argument list) will make a transition to state  $y_n$  at time  $t_n$ . Markov theory can be explained quite succinctly using joint probability functions as

$$P_{1|n-1}(y_n, t_n | y_{n-1}, t_{n-1}; y_{n-2}, t_{n-2}; \dots; y_1, t_1) = P_{1|1}(y_n, t_n | y_{n-1}, t_{n-1}), \quad (1.3)$$

that is to say that the transition probability of moving from one state to another does not depend on any previous state except the most recent state. Markov theory essentially erases the memory from the particular system in question. This means that we can write

$$P_2(y_1, t_1; y_2, t_2) = P_{1|1}(y_2, t_2 | y_1, t_1) P_1(y_1, t_1) \quad (1.4)$$

and can build up the whole Markov chain starting from the above expression. This is a particularly useful mathematical expression of a Markov process where it is clear to see that the probability of being in a particular state at a particular time depends only on the previous state and the transition probability from the old state into the new state. Considering the systems under study as finite Markov processes allows us to use the Markov method in the solution of the relevant quantities.

Once we have defined our system as a Markov process, our starting point is the stochastic master equation. In this work the focus will be on the solutions or analysis of the stochastic master equation where the probability distribution function  $[\rho(t)]$  governing the fate of a dif-

fusing particle on a Euclidean or fractal lattice is given by the following evolution equation<sup>2</sup> [26, 27]

$$\frac{d\rho_i(t)}{dt} = - \sum_{j=1}^N G_{ij} \rho_j(t). \quad (1.5)$$

Specifically,  $\rho_i(t)$  is the probability of the particle being at site  $i$  at time  $t$ , with

$$\rho_i(t=0) = \delta_{im}. \quad (1.6)$$

$G_{ij}$  is the transition rate of the probability to the site  $i$  from a neighboring site  $j$ . The overall  $\mathbf{G}$  matrix is linked to the  $N \times N$  Markov transition probability matrix<sup>3</sup>  $\mathbf{P}$  with elements  $p_{ij}$  via the relation

$$G_{ij} = [\delta_{ij} - p_{ij}]v_j \quad (1.7)$$

where  $v_j$  is the valency of site  $j$  and  $p_{ij}$  is the probability that the diffusing particle, conditional on being at site  $i$  at time  $t$ , will be at site  $j$  in the next displacement until terminating its walk (eventually) at one or more partially or completely absorbing traps. The  $p_{ij}$  reflect all of the constraints influencing the diffusional motion of the reactant. Consider a simple case where the particle is undergoing an unbiased, nearest-neighbor random walk. Then

$$p_{ii} = 0, \text{ and } p_{ij} = 1/v_j \text{ for } i \neq j \quad (1.8)$$

where  $v_j$  is the valency (number of nearest-neighbor sites) of site  $j$ .

The solutions to Eq. (1.5) are of the form

$$\rho_i(t) = \sum_k a_{ik} \exp(-\lambda_k t) \quad (1.9)$$

where the  $\lambda_k$  are the eigenvalues of  $\mathbf{G}$ . It can be shown that the mean walklength  $\langle n \rangle$  of the Markovian theory is related to the smallest eigenvalue  $\lambda_1$  of the above stochastic master equation via the relation

$$\langle n \rangle = v \lambda_1^{-1}. \quad (1.10)$$

In Chapter 2 we use the Markov method analytically and solve for  $\langle n \rangle$  utilizing Monte Carlo simulations. In Chapter 3 the Markov method is used along with Monte Carlo simulations as

<sup>2</sup>A similar but abbreviated form of Eq. (1.5) in matrix notation is commonly given as  $\dot{p}(t) = \mathbf{W}p(t)$  in ref. [25].

<sup>3</sup>See Appendix

well. A method which relies upon the solution of an inhomogeneous difference equation is also explored in Chapter 3 for the case where the reactants are situated on a  $1d$  lattice. An explicit example of the difference equation approach and the Markov approach is provided in the Appendix for the case of the 1WT with periodic boundary conditions in dimension  $d = 1$ .

In this work we will study reactions which occur between two reactive species. The principal focus will be on two kinetic schemes. The first is



in which  $T$  denotes a site occupied by an immobile target molecule (trap). The other scheme is



where  $A$  denotes a site occupied by a diffusing reactant molecule and  $S$  a free site. In this work, we shall refer to the scheme described by Eq. (1.12) as the “two-walker (2W) case”, while the kinetics described by Eq. (1.11) will be termed “one-walker plus trap (1WT) case”.

The mean walklength of a diffusing species before encountering a co-reactant is a natural measure of the time scale of a diffusion-reaction process. Let  $\langle n \rangle_1$  be the mean walklength before the irreversible reaction takes place in the 1WT case (Eq. (1.11)). Let  $\langle n \rangle_2$  be the corresponding quantity for the 2W case (Eq. (1.12)). The quantities  $\langle n \rangle_{1,2}$  are obtained by averaging over statistical realizations comprising all different initial configurations of both reaction partners. The smaller the value of  $\langle n \rangle_{1,2}$ , the higher the efficiency of the reaction.

## 1.2 Thesis organization

This thesis is comprised of two papers which are in press in *Physica A*. The work in Chapter 2 was performed principally by me with help from E. Abad. The writing and revising was performed by all four co-authors. The work in Chapter 3 was performed jointly by E. Abad and myself, with Abad doing the analytic work while the Monte Carlo simulations were performed by me. Again, the writing and revisions were performed by all four co-authors.

Chapter 2 examines how topology, dimensionality, and boundary conditions impact the efficiency of reaction considering two particle reactions. Two general classes of reactions are studied. Chapter 3 examines more closely synchronization effects where the two reactant mobility condition is even looser in the sense that at each time step there is a certain probability  $p$  that both walkers will move by one lattice space and a probability  $1 - p$  that only one walker will move and the other one will remain stationary. The problem is solved exactly in one dimension and in higher dimensions ( $2d$  and  $3d$ ) the problem is analyzed via Monte Carlo simulations.



## CHAPTER 2. Efficiency of encounter-controlled reaction between diffusing reactants in a finite lattice: topology and boundary effects

A paper published in *Physica A*<sup>1</sup>

Jonathan L. Bentz<sup>2</sup>, John J. Kozak<sup>3</sup>, E. Abad<sup>4</sup>, G. Nicolis<sup>5</sup>

### Abstract

The role of dimensionality (Euclidean versus fractal), spatial extent, boundary effects and system topology on the efficiency of diffusion-reaction processes involving two simultaneously-diffusing reactants is analyzed. We present numerically-exact values for the mean time to reaction, as gauged by the mean walklength before reactive encounter, obtained via application of the theory of finite Markov processes, and via Monte Carlo simulation. As a general rule, we conclude that for sufficiently large systems, the efficiency of diffusion-reaction processes involving two synchronously diffusing reactants (two-walker case) relative to processes in which one reactant of a pair is anchored at some point in the reaction space (one walker plus trap case) is higher, and is enhanced the lower the dimensionality of the system. This differential efficiency becomes larger with increasing system size and, for periodic systems, its asymptotic value may depend on the parity of the lattice. Imposing confining boundaries on the system enhances the differential efficiency relative to the periodic case, while decreasing the absolute efficiencies of both two-walker and one walker plus trap processes. Analytic arguments are

---

<sup>1</sup>*Physica A* 326/1-2 (2003) 55-68

<sup>2</sup>Graduate Student, Department of Chemistry, Iowa State University, Ames, Iowa 50011-3111

<sup>3</sup>Professor, Department of Chemistry, Iowa State University, Ames, Iowa 50011-3111

<sup>4</sup>Researcher, Center for Nonlinear Phenomena and Complex Systems, Université Libre de Bruxelles, C. P. 231, Bd. Du Triomphe, 1050 Brussels, Belgium

<sup>5</sup>Professor, Center for Nonlinear Phenomena and Complex Systems, Université Libre de Bruxelles, C. P. 231, Bd. Du Triomphe, 1050 Brussels, Belgium

presented to provide a rationale for the results obtained. The insight afforded by the analysis to the design of heterogeneous catalyst systems is also discussed.

## 2.1 Introduction

The influence of the interplay between spatial extent and system dimensionality on the reaction efficiency when reactants are undergoing random displacements on a finite lattice, with an irreversible reaction occurring on first encounter has attracted considerable interest over the last years [1, 2, 3, 4]. Whereas there is a vast literature dealing with the situation where one of the two reaction partners is anchored at some point in the reaction space [2, 3], a novel feature addressed more recently is when *both* reaction partners are allowed to diffuse simultaneously [1, 4]. This corresponds to the kinetic scheme



where  $A$  denotes a site occupied by a diffusing reactant molecule and  $S$  a free site, as opposed to the scheme



in which  $T$  denotes a site occupied by an immobile target molecule (trap). In this paper, we shall refer to the scheme described by Eq. (2.1) as the “two-walker (2W) case”, while the kinetics described by Eq. (2.2) will be termed “one-walker plus trap (1WT) case”.

In Refs. [1, 4], particular attention was focused on processes taking place on square-planar lattices subject to various boundary conditions. It was found that significant differences in reaction efficiency resulted depending on whether one or both reactants were diffusing. The objective of the present study is to inquire to what extent these results are generic and, if so, how they depend on the geometry of the support. The latter will be characterized, in turn, by the size, the embedding dimension, the intrinsic dimensionality, and by the topological invariants. Among these, for two-dimensional objects (surfaces) the Euler characteristic  $\chi = F - E + V$  where  $F$  is the number of faces,  $E$  the number of edges and  $V$  the number of vertices is especially significant. In each case, the role of the boundary conditions will also be assessed.

The mean walklength of a diffusing species before encountering a coreactant is a natural measure of the time scale of a diffusion-reaction process. Let  $\langle n \rangle_1$  be the mean walklength before the irreversible reaction takes place in the 1WT case (Eq. (2.2)). Let  $\langle n \rangle_2$  be the corresponding quantity for the 2W case (Eq. (2.1)). The quantities  $\langle n \rangle_{1,2}$  are obtained by averaging over statistical realizations comprising all different initial configurations of both reaction partners. The smaller the value of  $\langle n \rangle_{1,2}$ , the higher the efficiency of the reaction.

A point that will recur frequently in the following is that the reaction in the 2W case can occur via two different channels. In the first scenario, the two reaction partners happen to occupy adjacent sites on the lattice, and (with a certain probability) in their next, mutual displacement they undergo a collision. In the second channel, an intervening lattice site separates the two reactants and, in their subsequent motion (again, with a certain probability), both attempt to occupy that same (vacant) lattice site. As we shall see, one or both of these reaction channels can pertain, depending on the choice of boundary conditions and the parity of the total number of lattice sites  $N$ . Since both  $\langle n \rangle_1$  and  $\langle n \rangle_2$  depend on the characteristics of the lattice and on the boundary conditions, it will therefore be more appropriate to choose as a measure of the relative efficiency of the 2W process the ratio  $\Gamma \equiv \langle n \rangle_1 / \langle n \rangle_2$ .

There are both theoretical and experimental reasons for studying the influence of geometry and boundary conditions on the efficiency of diffusion-reaction processes. First, one would like to isolate effects that are independent of the boundaries of the domain in which the diffusion-reaction processes take place, and for this, periodic boundary conditions are usually imposed. Over the last several years, however, there has been an avalanche of experimental work published on the study of diffusion-reaction processes in microheterogeneous media [5] (micelles, clays, zeolites, etc.), with systems of finite extent (nanosystems) showing non-classical behavior (i.e., departures from “mean field” behavior). Therefore, in the present study we have also examined in tandem with periodic boundary conditions, systems subject to confining boundary conditions. Specifically, in adopting confining boundary conditions, one imposes the condition that if a diffusing particle attempts to exit the lattice from a given boundary site, it is simply reset at that boundary site.

The calculations performed in this paper are of two kinds. First, we use the theory of finite Markov processes to compute  $\langle n \rangle_1$  and  $\langle n \rangle_2$ , for small, finite lattices subject either to periodic or confining boundary conditions. The advantage of this approach is that one obtains numerically-exact solutions to the problem under study and, in certain cases, one can construct closed-form analytic solutions. Mirroring this, we also perform Monte Carlo calculations, first validated by comparison with the Markov results and then used to analyze systems of large spatial extent.

The plan of this paper is as follows. In Secs. 2.2–2.4, we consider successively lattices of Euclidean dimension  $d = 1, 2$  and  $3$ , as well as the Sierpinski gasket, a lattice of fractal dimension  $D = \ln 3 / \ln 2$ . The influence of size effects, boundary conditions and other related topological features such as the connectivity and the Euler characteristic is discussed in each dimension. The main conclusions are summarized in Sec. 2.5.

## 2.2 Euclidean dimension, $d = 1$

The 1WT problem on a  $d = 1$  finite lattice subject to periodic boundary conditions was solved by Montroll [6] analytically. The result he found was:

$$\langle n \rangle_1 = \frac{N(N+1)}{6}, \quad (2.3)$$

where  $N$  is the total number of sites in the lattice.

The solution for the case of two walkers in  $d = 1$  for a lattice subject to periodic boundary conditions can be obtained in closed form by formulating the problem as a classical ruin problem and solving the correspondence difference equations [7]. The result is

$$\langle n \rangle_2 = \begin{cases} N(N+1)(N+2)/12(N-1) & \text{for } N \text{ even} \\ (N+1)(N+3)/12 & \text{for } N \text{ odd} \end{cases} \quad (2.4)$$

This result can also be obtained via the theory of finite Markov processes by calculating numerically-exact values of  $\langle n \rangle_2$  for a series of  $d = 1$  lattices. From these results patterns can be recognized from which one can construct the above closed-form analytic solution.

We notice a difference in the expression for  $\langle n \rangle_2$  for even and odd values of  $N$  also found in Refs. [1, 4] and which will turn out to become more pronounced in higher dimensions. We find

that this *qualitative* difference in behavior between even and odd lattices is always manifested if periodic boundary conditions are considered, but not if confining boundary conditions are imposed. This behavior can be rationalized by examination of small odd and even lattices. The key to this difference is in the reaction mechanism, which happens either via nearest-neighbor collision (NNC) or via same-site occupation (SSO).

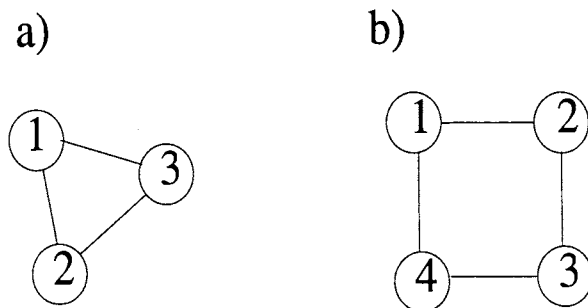


Figure 2.1 Periodic  $d = 1$  lattices with a)  $N = 3$  and b)  $N = 4$ .

Consider the two periodic lattices of size  $N = 3$  and  $4$  shown in Figs. 2.1a and b. For  $N = 3$ , assume that we place a walker on site 1 and another one on site 3. Concerned only with the concerted motions leading to reaction, one can see that reaction takes place by SSO if both walkers jump to site 2, or by NNC if they attempt to exchange positions. Thus, both reaction channels are open. Now consider the periodic  $N = 4$  lattice and place again the walkers on sites 1 and 3. The reaction can proceed by SSO if both walkers jump to site 2 or site 4 after one time step. Otherwise, they will always be two sites apart, essentially following each other in the lattice. This means that starting with the initial configuration of walkers on sites 1 and 3, the only allowed reaction channel is SSO. On the other hand, if sites 1 and 2 are chosen as the initial positions of the walkers, or more generally any adjacent pair of sites, reaction can only occur by NNC. This is true because any concerted motion will either lead to NNC or the walkers will remain nearest-neighbors after each time step. More generally, it is easily seen that for an even lattice only one of the reaction channels is active for any given initial configuration, whereas for odd lattices, both can take place. This phenomenon will hereafter be referred to as the “even-odd effect”.

We next consider the 1WT and the 2W problems in a  $d = 1$  lattice subject to confining boundary conditions. From Markov theory, one obtains for the 1WT case:

$$\langle n \rangle_1 = \frac{N(N+1)}{3}. \quad (2.5)$$

According to this formula, the reaction efficiency is reduced by a factor of 2 with respect to the periodic case described by Eq. (2.3) for all system sizes. The reason is that the lattice with confining boundaries and a trap  $T$  can be decomposed into two disconnected periodic lattices, each of them with a trap, since the parts of the lattice on either side of  $T$  do not communicate.<sup>6</sup> This equivalence is illustrated in Fig. 2.2a for a confining lattice with  $N = 4$ . The weighted size of all equivalent periodic lattices resulting from the different positions of the trapping site  $T$  is larger than  $N$ . Similar arguments are expected to apply in higher dimensions. Thus, confinement always reduces the efficiency of the reaction.

As for the 2W problem, no closed form expression similar to Eq. (2.4) has yet been derived for the case of confining boundary conditions. However, values of  $\langle n \rangle_2$  for this case could be calculated numerically using both the Markov method and Monte Carlo simulations. As in the 1WT case, the efficiency is smaller than in the periodic lattice case, but the increase in  $\langle n \rangle_2$  when confinement is imposed is smaller than the factor of 2 found in the 1WT case for all values of the lattice size  $N$  larger than two,<sup>7</sup> approaching a value close to 1.70 from below in the asymptotic limit (not shown). Once more, an equivalence with the periodic case can be established here. However, the difference with the 1WT case is that now the size of the equivalent periodic lattices fluctuates in time, as it depends on the instantaneous distance between the walkers. These lattice size fluctuations possibly explain why the loss of efficiency is smaller in the 2W case when one switches from periodic to confining boundary conditions.

We notice that no even-odd effect is to be expected in the confining case. This is illustrated in Fig. 2.2b with two walkers initially placed on sites 1 and 3. Obviously SSO occurs if both walkers jump to site 2. If both walkers jump to the left, then the walker on site 3 will jump to site 2, but the walker on site 1 will not move. Both walkers occupy now adjacent sites and NNC

---

<sup>6</sup>For the special case where the trap is placed at an edge site, the confining lattice reduces to a single rather than to two periodic lattices.

<sup>7</sup>For  $N = 2$ , a confining lattice is even more effective than a periodic one.

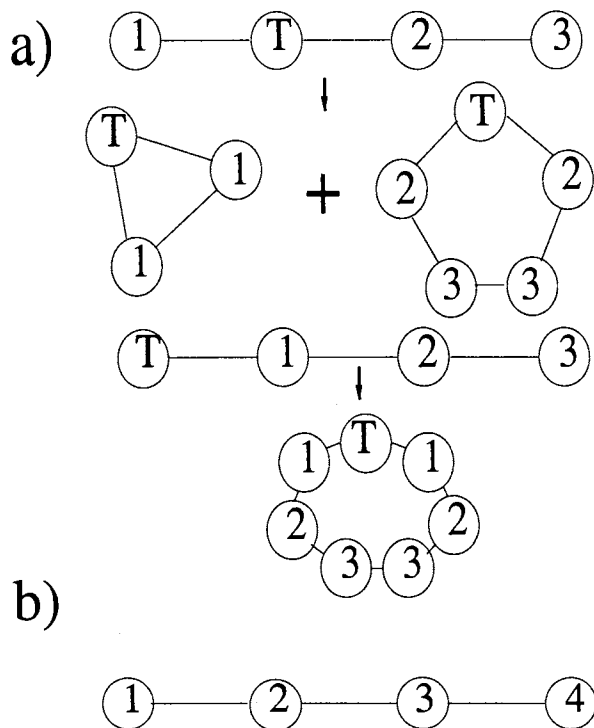


Figure 2.2 a) Correspondence between confining and periodic boundary conditions for the two symmetry-distinct trap configurations in a confining 4-site lattice. Sites with same numbers are symmetry-equivalent. b) Four site confining lattice.

becomes possible at the next time step. For the other symmetry-distinct initial configuration with walkers at sites 1 and 2, one can formulate an analogous sequence of jumps leading to SSO. Thus, for a given initial condition, the imposition of confining boundary conditions allows both reaction channels on an even-site lattice, whereas with periodic boundary conditions only one of them is realized.

Figure 2.3 depicts the behavior of the relative efficiency  $\Gamma$  defined in the Introduction as a function of the lattice size  $N$ . It reveals an important feature, seen for all Euclidean lattices studied regardless of dimension or class of boundary conditions.<sup>8</sup> The curve  $\Gamma$  vs.  $N$  exhibits a steep increase initially with increase in  $N$  but then it “flattens out” and appears to be saturating at a particular limiting value  $\Gamma_\infty \equiv \lim_{N \rightarrow \infty} \Gamma$ . The limiting value  $\Gamma_\infty$  is different

<sup>8</sup>The sole exception is the  $d = 3$  cubic lattice subject to confining boundary conditions; see Section 2.4.1.

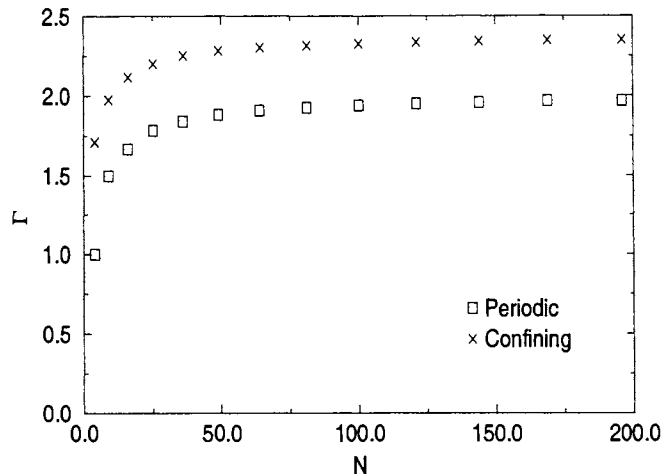


Figure 2.3  $\Gamma$  vs.  $N$  in  $d = 1$ . The curve for the periodic case is generated from the exact analytical results and the data for the confining case is from Monte Carlo simulations.

for different dimensions, but the same steep increase followed by a very gradual increase to a limiting value is found. For the periodic case in  $d = 1$ , the numerical evidence suggests that the curve is approaching a value close to 2; upon inspection of the analytic form of the solutions given by Eqs. (2.3) and (2.4) one sees that the value in the limit of large  $N$  is exactly 2. This is related to the fact that, due to the translational invariance of the lattice, the 2W problem can be reduced to an equivalent 1WT problem, and the effective diffusion coefficient for the latter becomes twice as large in the large  $N$  limit [7].

A second feature revealed by a closer examination of the analytic form for  $\Gamma$  in the periodic case is that the increase with size is staircase-like since  $\Gamma$  takes the same value for two consecutive odd and even values of  $N$  [7]. This consequence of the even-odd effect characteristic of the periodic case is not seen at the scale of resolution of Fig. 2.3 and is actually unimportant for the qualitative behavior over sufficiently large  $N$  intervals. Unlike toroidal (periodic) lattices in higher dimensions, the even-odd effect in one dimension does not lead to different asymptotic values  $\Gamma_{\infty}^{even}$  and  $\Gamma_{\infty}^{odd}$  depending on whether only even or only odd lattices are considered for the computation of the respective walklengths.



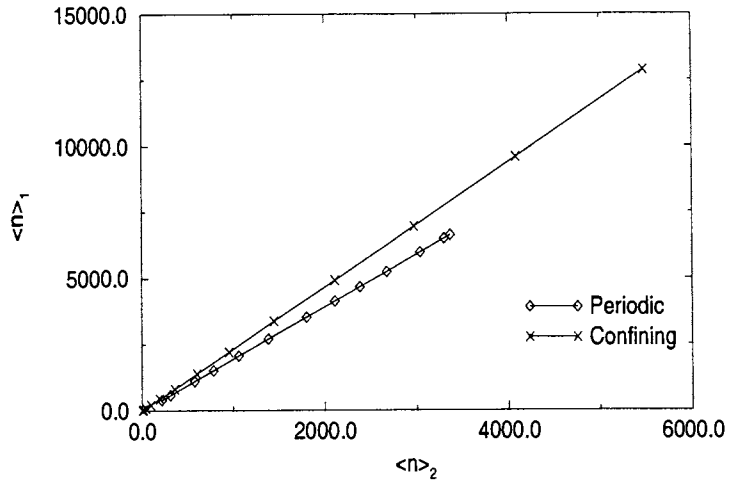


Figure 2.4  $\langle n \rangle_1$  vs.  $\langle n \rangle_2$  in  $d = 1$ . The slopes of the best-fit lines are: Periodic = 1.97 and Confining = 2.35.  $N_{\min} = 49$  for the periodic case ( $N_{\min}$  is the smallest data point used in the calculation of the best fit curve.) Both curves have R values of greater than 0.999.

In general, plotting the  $\langle n \rangle_1$  vs. the  $\langle n \rangle_2$  data for sufficiently large values of  $N$ , as displayed in Fig. 2.4, is a convenient way of determining the saturation value  $\Gamma_{\infty}$ . The slope value from a least-squares curve fit for periodic lattices is 1.97, in good agreement with the exact analytical value, and 2.35 for confining lattices.

### 2.3 Euclidean dimension, $d = 2$

A square-planar lattice with periodic boundary conditions is topologically equivalent to a torus and has an Euler characteristic  $\chi$  of 0. Results in  $d = 2$  have already been reported for the case of a square-planar lattice subject to periodic boundary conditions [1]. Figure 2.5 shows clearly the behavior of  $\Gamma$  in the large lattice limit, which is different for odd and even lattices. In Ref. [1], analytical evidence was provided to show that the asymptotic limit of  $\Gamma$  for odd lattices is  $\Gamma_{\infty}^{odd} = \sqrt{2}$ .

As mentioned in the Introduction, surfaces are characterized topologically not only by their Euclidean dimension but also by their Euler characteristic. Thus, it is also of interest to

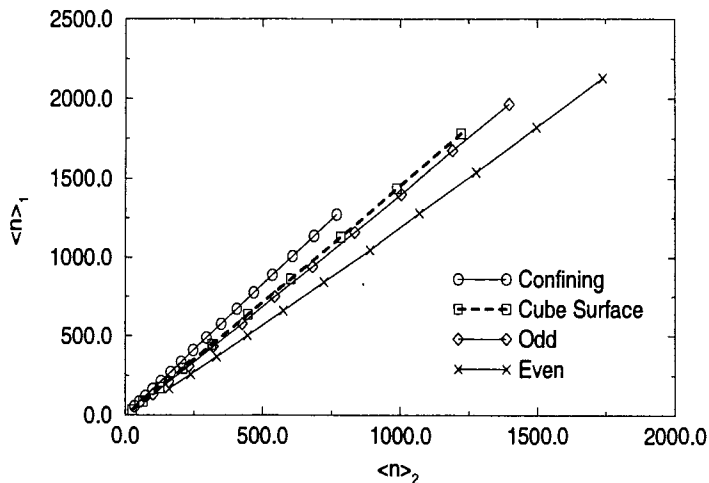


Figure 2.5  $\langle n \rangle_1$  vs.  $\langle n \rangle_2$  in  $d = 2$ . The slopes of the best-fit lines are: Confining = 1.66, Even = 1.25, Odd = 1.42, Cube Surface = 1.47. All data are calculated from simulations. The values of  $N_{\min}$  are: Confining = 25, Even = 100, Odd = 81, Cube Surface = 24. All R values are greater than 0.999.

consider non-toroidal surfaces with Euler characteristic  $\chi \neq 0$ . In particular, for the sphere and the family of polyhedra homeomorphic to it, one has  $\chi = 2$ . We shall consider two examples, the first of which is the case of diffusion-reaction processes on the surface of the Platonic solids. One of the reasons motivating the study of such polyhedral systems is that they mimic some features of real-world solid catalysts where the reaction takes place on particular crystallographic faces of the solid. In earlier work [8], the vertices of the Platonic solids were used as the allowable particle positions. The movement of each particle was permitted along any adjoining edge. In the present study, we report the results of the calculation using the faces of the Platonic solids; the particle moves from face to adjacent face, crossing only one edge at each time step. The relationship between these two calculations is reciprocal. In formal language, two polyhedra are dual if the number of faces of one of them equals the number of vertices of the other, and vice versa [9]. Recall that the tetrahedron has 4 faces and 4 vertices and both faces and vertices have a valency of 3. The octahedron has 8 faces and 6 vertices,

and the hexahedron (cube) has 6 faces and 8 vertices. The valency of the octahedron faces is 3 as is the valency of the cube vertices. Likewise, the valency of the octahedron vertices is 4 as is the valency of the cube faces. Performing the calculation on the faces of the octahedron is equivalent to the calculation on the vertices of the cube, and the same reciprocal relation holds true when examining the icosahedron and the dodecahedron. Table 2.1 shows results for  $\langle n \rangle_1$  and  $\langle n \rangle_2$  on the Platonic solids. As can be seen, with the exception of the octahedron,  $\Gamma$  increases with  $N$ , in line with the results for the square planar lattice.

Object	$N$	valency	$\langle n \rangle_1$	$\langle n \rangle_2$	$\Gamma$
Tetrahedron	4	3	3	3	1
Hexagonal Lattice	4	3	3.6667	4.8214	0.7606
Octahedron	8	3	8.2857	9	0.9206
Hexagonal Lattice	8	3	8.2857	9	0.9206
Icosahedron	20	3	28.8421	21.0955	1.3672
Hexahedron	6	4	5.2	5.0182	1.0362
Square Lattice	6	4	5.7714	5.8915	0.9796
Dodecahedron	12	5	12.7273	11.1676	1.1397

Table 2.1 Analytic results for Platonic solids and planar analogues with periodic boundary conditions

It is instructive to view the results of the Platonic solids in tandem with their planar analogues. The tetrahedron, octahedron and hexahedron can be placed in correspondence with periodic planar lattices with the same valency and same value of  $N$ ; the dodecahedron and icosahedron have no periodic, planar analogues. In correspondence with the tetrahedron and octahedron we constructed hexagonal lattices for comparison, while the hexahedron was compared with a  $2 \times 3$  square-planar lattice. The tetrahedron and hexahedron have smaller values than their planar analogues for the walklengths  $\langle n \rangle_1$  and  $\langle n \rangle_2$  but larger values of  $\Gamma$ . Surprisingly all the walklength values for the octahedron and the 8-site hexagonal lattice are identical. Upon further examination of this degeneracy, one finds that the values are identical because the connectivity of the octahedron is identical, site by site, with the connectivity of the 8-site periodic hexagonal lattice. These calculations show, surprisingly, that the connectivity of the lattice seems to play a relatively more important role than the Euler characteristic in

determining the value of the mean walklength.

We also examined the influence of imposing confining boundary conditions on the planar lattice analogues of the Platonic solids. Owing to the fact that the connectivity of sites on the boundary of these (finite) lattices changes, the values of  $\langle n \rangle_1$  and  $\langle n \rangle_2$  change. The values of  $\langle n \rangle_2$  for all three planar analogues are only slightly larger than for the case where periodic boundary conditions are imposed. On the other hand, the values of  $\langle n \rangle_1$  are considerably larger than the values of  $\langle n \rangle_1$  calculated for periodic boundary conditions; for the  $N = 4$  hexagonal lattice, the  $N = 8$  hexagonal lattice and the  $N = 2 \times 3$  square-planar lattice, the value of  $\langle n \rangle_1$  increases by a factor of 3, 4 and 2, respectively. Thus, in small systems, changes in the boundary conditions have a significant effect on the calculation of  $\langle n \rangle_1$ , but less so on the calculation of  $\langle n \rangle_2$ . Overall, the influence of boundary conditions on both the 1WT and 2W cases for these planar analogues of the Platonic solids is more drastic than is the case for a (small)  $d = 1$  lattice. This is reflected in the value of  $\Gamma$ , which increases by a larger factor here than in the  $d = 1$  case when confining boundary conditions are imposed.

In order to emulate large-size systems, we have studied diffusion-reaction processes on the surface of a cube, which is also of Euclidean dimension  $d = 2$  and Euler characteristic  $\chi = 2$ . The particle is confined to the surface, and each face of the cube is divided into a  $N \times N$  square planar grid so that there are  $N \times N$  accessible sites on each face. The total number of sites is  $N \times N \times 6$ . Note that for  $N = 1$  the previous case of an hexahedron is recovered. The valency of each site is exactly four, keeping in mind that some movements of the walker will take it to a different face.

Figure 2.5 summarizes the  $d = 2$  results in the large lattice limit. It is seen that, on the surface of a cube, the differential efficiency  $\Gamma$ , given by the slope of the curve  $\langle n \rangle_1$  vs.  $\langle n \rangle_2$ , is larger than on a periodic but smaller than on a confining square planar lattice. As expected, the efficiency of 1WT processes is once again decreased in a more pronounced way when confinement is imposed. The even-odd effect is not seen for processes on the surface of a cube or for planar lattices subject to confining boundary conditions. On the cube, an argument analogous to the one put forth for  $d = 1$  applies, except that the walkers on the

cube surface have two additional degrees of freedom. However, this has no influence on the fact that, irrespective of the starting configuration, both NNC and SSO may still take place because of the the walkers' ability to traverse edges and thereby migrate to different faces of the cube.

## 2.4 Higher dimensions and fractal structures

### 2.4.1 Euclidean dimension, $d = 3$

Numerically-exact results have been reported previously [10, 11] for the 1WT case on a  $d = 3$  cubic lattice subject to periodic boundary conditions. We have extended this study to calculate  $\langle n \rangle_1$  and  $\langle n \rangle_2$  for both periodic and confining boundary conditions by means of Monte Carlo simulations. In  $d = 3$ , the even-odd effect is even more pronounced than in the square-planar lattice case, as may be seen in Fig. 2.6. From the least-square fits we infer  $\Gamma_\infty^{\text{even}} = 0.72$  and  $\Gamma_\infty^{\text{odd}} = 1.22$ . This suggests that the even-odd effect is enhanced with increasing dimensionality of the hypercubic lattice. Note also that  $\Gamma_\infty < 1$  for even lattices, the only case where the differential efficiency goes below unity except for the octahedron.

For confining boundary conditions, another significant result for  $d = 3$  is shown in Fig. 2.7. As is evident,  $\Gamma$  approaches its limiting value *from above*, and  $\Gamma_\infty$  is found to be about 1.42 in this case. In all previous cases, namely the  $d = 1$  and 2 cases with both types of boundary conditions, the graphs had the general features of Fig. 2.3, approaching  $\Gamma_\infty$  from below.

### 2.4.2 Fractal dimension, $D = \ln 3 / \ln 2$

From the results presented for the cases  $d = 1$ , the  $d = 2$  square-planar lattice, and  $d = 3$  cubic lattice subject to confining boundary conditions, one can infer that, with increasing dimensionality  $d$  of the lattice,  $\Gamma_\infty$  decreases monotonically taking the values 2.35, 1.66 and 1.42, respectively, for  $d=1, 2$  and 3. In order to assess further the role of dimensionality and of confinement, one can next consider the case of a Sierpinski gasket, whose ramified self-similar structure is described by an intrinsic non-integer dimension  $D = \ln 3 / \ln 2 \simeq 1.585$ . The gasket can be constructed hierarchically as a limit of successive generation gaskets. Each

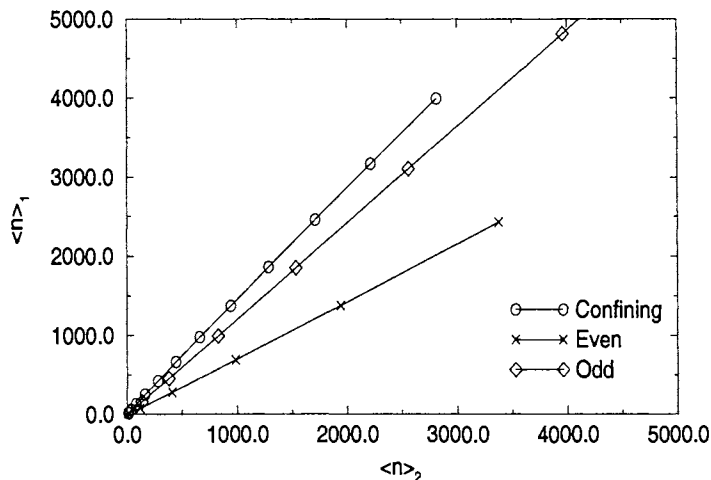


Figure 2.6  $\langle n \rangle_1$  vs.  $\langle n \rangle_2$  in  $d = 3$ . The slopes of the best-fit lines are: Odd = 1.22, Even = 0.72, Confining = 1.42. All data are calculated from simulations.  $N_{\min} = 8$  for all the curves with all R values greater than 0.999.

generation gasket is characterized by an index  $i$ . The  $i = 0$  generation is an equilateral triangle whose 3 vertices play the role of lattice sites, i.e. allowable reactant positions. The  $i = 1$  generation can be constructed by appending to each of the bottom vertices of the primary triangle an additional equilateral triangle so that the upper vertices of the appended triangles are identical with the bottom vertices of the primary one and the appended triangles have a common bottom vertex. The  $i = 2$  generation is constructed by performing the same procedure on the resulting structure, i.e. appending twice the same structure at its bottom, and so on. Thus, at a given generation step, the number of identical substructures increases by three while the linear size doubles, yielding the above value of  $D$  for the Sierpinski gasket obtained when  $i \rightarrow \infty$ . For each generation, the lattice sites are identified with the three apex vertices located at the outmost corners of the corresponding gasket and with the common vertices of any pair of adjacent triangles in the gasket. The number of sites in the  $i$ th generation gasket is  $N = N(i) = (3/2)(3^i + 1)$ .

The gasket shares some common features with a square-planar lattice. First, the embedding

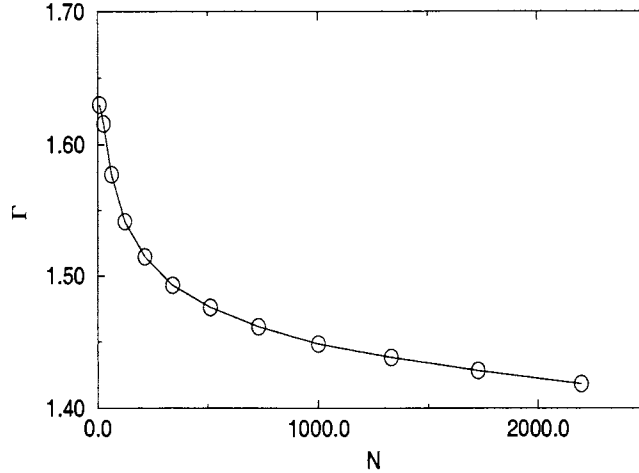


Figure 2.7  $\Gamma$  vs.  $N$  in  $d = 3$  subject to confining boundary conditions; all data are calculated from simulations.

dimension is the same, viz.  $d = 2$ . Secondly, except for the vertex sites on the gasket, the valency of all other sites is  $v = 4$ ; increasing the size of the gasket decreases the fraction of lattice sites not having a valency of 4. All sites on a square-planar lattice subject to periodic boundary conditions have a valency  $v = 4$ . On imposing confining boundary conditions on the square-planar lattice, all interior sites will have valency  $v = 4$ , vertex sites will have valency  $v = 2$  and boundary sites will have valency  $v = 3$ ; the percentage of vertex and boundary sites on a square-planar lattices also decreases with increase in lattice size. Thus, both for the gasket and for a finite square-planar lattice subject to confining boundary conditions, the relative importance of interior sites on the statistics increases with increasing lattice size. Finally, one can easily convince oneself that in the 2W case both the SSO and NNC channels can take place for any given configuration of the walkers on the gasket, so no even-odd effect is expected here either.

In view of the above resemblances, it is interesting to inquire to what extent the results obtained for the relative efficiency  $\Gamma$  on the gasket are similar to those for the square lattice with confining boundary conditions. To this end,  $\langle n \rangle_1$  and  $\langle n \rangle_2$  and their ratio were calculated using

the theory of finite Markov processes for  $N = 6, 15,$  and  $42$  and via Monte Carlo simulations for all generations up to  $N = 3282$ . For the 1WT case, a closed-form analytic expression for the walklength is already available if the trap is maintained at one of the apex vertices of the  $i$ th generation gasket, namely [12]

$$\langle n \rangle_{1,a} = \frac{3^i 5^{i+1} + 4(5^i) - 3^i}{3^{i+1} + 1}. \quad (2.6)$$

In performing Monte Carlo simulations, the amount of computing time can increase dramatically with increase in gasket size  $N$  thus limiting the number of statistical realizations  $n_{real}$ . In the 1WT case, each realization comprises all sets of possible configurations for the walker and the trap, while in the 2W case, each realization comprises all sets of possible configurations for the two indistinguishable walkers. The analytic expression of  $\langle n \rangle_{1,a}$  given in Eq. (2.6) was used to test the accuracy of MC results for gasket sizes  $N > 123$ , where the Markovian approach becomes cumbersome due to the size of the relevant transition matrices. It was found that, as  $N$  is increased, the number of realizations required to reach a given accuracy in  $\langle n \rangle_{1,a}$  with respect to the exact result given by (2.6) decreases significantly. For all values of  $n_{real}$  given in Table 2.2, the relative error turned out to be  $< 0.4\%$  (data not shown). Therefore, the results for  $\langle n \rangle_1$  and  $\langle n \rangle_2$  for large  $N$  displayed in Table 2.2 seem reliable enough to describe correctly the qualitative behavior of the efficiencies.

$i$	$N$	Markov Results			Monte Carlo Results			
		$\langle n \rangle_1$	$\langle n \rangle_2$	$\Gamma$	$\langle n \rangle_1$	$\langle n \rangle_2$	$\Gamma$	$n_{real}$
1	6	6.5	4.3860	1.4820	6.500	4.386	1.482	$10^7$
2	15	25.6857	16.0957	1.5958	25.686	16.096	1.596	$10^7$
3	42	118.0582	68.9220	1.7129	118.06	68.94	1.713	$10^6$
4	123	-	-	-	578.18	315.90	1.830	$10^5$
5	366	-	-	-	2886.1	1500.9	1.923	$10^3$
6	1095	-	-	-	14465.3	7282.9	1.986	10
7	3282	-	-	-	72512.6	35724.1	2.029	1

Table 2.2 Walklength results for successive Sierpinski generation gaskets.

Although the convergence to a hypothetical saturation value is very slow in  $N$ , one notices from Table 2.2 that  $\Gamma$  appears to exceed the value 2 with increasing  $N$ , in contrast to the result  $\Gamma_\infty = 1.66$  for a confining square lattice. Assuming that  $\Gamma$  keeps on increasing monotonically



with the gasket size  $N$ , a question of interest is whether  $\Gamma$  approaches a saturation value less than the value 2.35 found for a  $d = 1$  confining lattice, or whether the asymptotic value remains between the values 1.66 and 2.35, as one might expect in view of the monotonic decrease of  $\Gamma_\infty$  with decreasing dimensionality referred earlier.

## 2.5 Conclusions

In this work, results, both analytic and numerical, on the role of boundary effects and of geometric factors such as size, dimensionality and topological invariants on the efficiency of encounter-controlled reactions have been obtained. Values for the mean walklengths  $\langle n \rangle_1$  and  $\langle n \rangle_2$  for the 1WT and the 2W case as well as the relative efficiency  $\Gamma$  have been computed both for large lattices and small size systems.

The relevance of considering in detail systems of restricted spatial extent is increasing, as it is nowadays realized that heterogenous catalytic processes of great importance take place on single crystallographic faces of solid catalysts where they can involve only a few tens of particles. Despite the fact that the numerical values obtained in this work for small systems are not universal, some universal trends of a different kind have nevertheless been observed, e.g. the dependence (increasing, monotonic, etc.) of  $\Gamma$  on valency, connectivity and boundary conditions. In general, one has  $\Gamma > 1$ , implying that the reactive efficiency of two moving reactants is greater than a diffusing plus an immobile one.

Turning now to large-size systems, our results show that  $\Gamma$  increases with increasing lattice size until it reaches a well-defined limiting value  $\Gamma_\infty$ . For a given lattice geometry, this value decreases with increasing dimensionality. With the exception of the even cubic lattice,  $\Gamma_\infty > 1$ .

For Euclidean lattices of square-planar or cubic symmetry and subject to periodic boundary conditions the value of  $\Gamma_\infty^{odd}$  is exactly 2 and  $\sqrt{2}$  in one<sup>9</sup> and two dimensions respectively, and about 1.22 in three dimensions. One is tempted to advance that this last number is actually within the precision afforded by the simulations just  $\sqrt{(3/2)}$ . Now, 1,  $\sqrt{2}$  and  $\sqrt{3}$  are the

---

<sup>9</sup>In the diffusive limit, it can be shown that the diffusion coefficient for the relative motion of both reactants is twice as large in the 2W case [7]. Discrepancies from this value for small systems are due to the discreteness of the lattice. Possibly similar arguments hold in higher dimensions.

natural metrics of the lattices here considered in, respectively, 1, 2 and 3 dimensions. The results for  $\Gamma_{\infty}^{odd}$  could then be particular cases of a universal expression: the ratio of the maximum distance that two simultaneously moving reactants can traverse in one time unit before they react or find themselves in nearest neighbor positions, over the analogous quantity for the one reactant plus trap case. Further work is necessary to assert the validity of this conjecture and to understand why it manifests itself only for odd lattices.

For a given system size, the 1WT and the 2W reaction efficiency becomes less efficient when confinement is introduced, but the decrease in efficiency is smaller for the 2W case, leading to an increased value of  $\Gamma$  with respect to the periodic case. This boundary effect appears to become less significant with increasing system size, although it is not completely absent in the thermodynamic limit.

The questions raised in this work and the results obtained constitute potentially useful elements in the important problem of optimal design of the microreactors nowadays involved in chemical kinetics under nanoscale conditions. For instance, as seen in Sec. 2.3, a small catalytic surface in the form of a sphere or of a hexahedral surface homeomorphic to it ( $\chi = 2$ ) would enhance the reaction efficiency as compared to a surface homeomorphic to a torus ( $\chi = 0$ ). These observations highlight the need to incorporate in the design such aspects as the geometry of the microreactor, which can enhance an increasingly effective mixing of the reactants and hence an increased efficiency of the reaction itself. Finally, the role of the kinetics (linear vs. nonlinear) in modulating or enhancing the importance of such factors is certainly a problem worth addressing and this study is underway.

## Acknowledgements

It is a pleasure to thank Dr. M. Plapp for valuable suggestions concerning the hierarchical construction of the Sierpinski gasket. This work is supported by a NATO Cooperative linkage grant PST.CLG.977780 and by the European Space Agency under contract number 90043.

## References

- [1] J.J. Kozak, C. Nicolis, G. Nicolis, *J. Chem. Phys.* 113 (2000) 8168.
- [2] J.J. Kozak, *Adv. Chem. Phys.* 115 (2000) 245.
- [3] G.H. Weiss, *Aspects and Applications of the Random Walk*, North-Holland, New York/Amsterdam, 1994.
- [4] C. Nicolis, J.J. Kozak, G. Nicolis, *J. Chem. Phys.* 115 (2001) 663.
- [5] A.V. Barzykin, K. Seki, M. Tachiya, *Adv. Coll. Inter. Sci.* 89-90 (2001) 47.
- [6] E. Montroll, *J. Math. Phys.* 10 (1969) 753.
- [7] E. Abad, G. Nicolis, J.L. Bentz, J.J. Kozak, *Physica A* 326/1-2 (2003) 69.
- [8] P.A. Politowicz, J.J. Kozak, *Proc. Natl. Acad. Sci. USA.* 84 (1987) 8175.
- [9] M. Henle, *A Combinatorial Introduction to Topology*, W.H. Freeman and Company, San Francisco, 1979.
- [10] C.A. Walsh, J.J. Kozak, *Phys. Rev. B.* 26 (1982) 4166.
- [11] C.A. Walsh, J.J. Kozak, *Phys. Rev. Lett.* 47 (1981) 1500.
- [12] J.J. Kozak, V. Balakrishnan, *Phys. Rev. E.* 65 (2002) 021105.

## CHAPTER 3. Synchronous vs. asynchronous dynamics of diffusion-controlled reactions

A paper published in *Physica A*<sup>1</sup>

E. Abad<sup>2</sup>, G. Nicolis<sup>3</sup>, Jonathan L. Bentz<sup>4</sup>, John J. Kozak<sup>5</sup>

### Abstract

An analytical method based on the classical ruin problem is developed to compute the mean reaction time between two walkers undergoing a generalized random walk on a  $1d$  lattice. At each time step, either both walkers diffuse simultaneously with probability  $p$  (synchronous event) or one of them diffuses while the other remains immobile with complementary probability (asynchronous event). Reaction takes place through same site occupation or position exchange. We study the influence of the degree of synchronicity  $p$  of the walkers and the lattice size  $N$  on the global reaction's efficiency. For odd  $N$ , the purely synchronous case ( $p = 1$ ) is always the most effective one, while for even  $N$ , the encounter time is minimized by a combination of synchronous and asynchronous events. This new parity effect is fully confirmed by Monte Carlo simulations on  $1d$  lattices as well as for  $2d$  and  $3d$  lattices. In contrast, the  $1d$  continuum approximation valid for sufficiently large lattices predicts a monotonic increase of the efficiency as a function of  $p$ . The relevance of the model for several research areas is briefly discussed.

---

<sup>1</sup>*Physica A* 326/1-2 (2003) 69-87

<sup>2</sup>Researcher, Center for Nonlinear Phenomena and Complex Systems, Université Libre de Bruxelles, C. P. 231, Bd. Du Triomphe, 1050 Brussels, Belgium

<sup>3</sup>Professor, Center for Nonlinear Phenomena and Complex Systems, Université Libre de Bruxelles, C. P. 231, Bd. Du Triomphe, 1050 Brussels, Belgium

<sup>4</sup>Graduate Student, Department of Chemistry, Iowa State University, Ames, Iowa 50011-3111

<sup>5</sup>Professor, Department of Chemistry, Iowa State University, Ames, Iowa 50011-3111

### 3.1 Introduction

Recently, the modelling of diffusion-controlled reactions on lattices has attracted renewed interest due to synergies with some research areas like e.g. heterogeneous catalysis [1, 2], trapping problems [3], spin models [4], game theory [5], population dynamics [6] or biological problems [7]. An issue common to these systems is the important role played by the coexistence of different intrinsic time scales, the lattice characteristics (size and dimensionality) and many-body effects. The interplay of these ingredients may strongly affect the efficiency with which statistical processes such as front propagation on catalytic substrates, the spread of an infection, kink propagation in magnetic systems, or exciton trapping in photosynthetic cells take place. In order to obtain analytical insight for such systems, it is often necessary to make simplifying assumptions which nevertheless preserve their main generic features.

In this spirit, a prototypical diffusion-reaction system consists of two interacting walkers performing nearest neighbor jumps on a lattice [8]. The walkers are assumed to react with each other whenever they meet at the same lattice site or attempt to exchange positions. Each of such “encounters” results in instantaneous reaction, the process therefore being diffusion-controlled. Regardless of the particular outcome of the reaction, a measure for its efficiency will be clearly given by the mean encounter time of both walkers.

In a pioneering work, Montroll investigated a simplified version of the problem in which one of the walkers is stationary, thereby playing the role of a fixed trap [9]. In a recent article [10], Montroll’s results have been extended with the help of a Markovian method to account for the possibility of simultaneous displacement of the walkers. In the present work, the problem is further extended to the case in which the motion of the walkers consists of a random sequence of two different events: at each tick of the clock, a synchronous event takes place with probability  $p$ , i.e., both walkers hop simultaneously to randomly chosen nearest neighbor sites. Alternatively, an asynchronous event takes place with probability  $1 - p$ , i.e. one of the walkers performs a nearest neighbor jump while the other remains immobile. Thus, the parameter  $p$  interpolates between the one walker plus trap case studied by Montroll ( $p = 0$ ) and the case of two simultaneously moving walkers ( $p = 1$ ). A central question we shall investigate here

concerns the influence of the degree of synchronicity  $p$  of the walkers and the size  $N$  of the lattice in which they are embedded upon the reaction's efficiency.

Our model may be of interest in several contexts. One can e.g. easily accommodate it to allow for events in which both walkers remain immobile in the original reference frame. Thus, three qualitative different joint events become possible for the two-walker system, which can e.g. be interpreted as resulting from a combination of two internal states for each of the walkers, namely a diffusing and an immobile state. Such two-state random walks [11, 12, 13] are frequently used to model chromatographic [14] or electrophoretic separation processes, in which the propagation of charged particles in an external field may be occasionally stopped by entanglement with the molecules of the substrate. Such systems, along with hopping models for transport and recombination of carriers in solids [15, 16, 17], might provide additional motivation for considering a generalized version of the random walk.

A different approach suggests to regard the fluctuations in the diffusivity of the walkers as a result of random fluctuations of lattice sites switching between a conducting and a stopping state, whereby the translational invariance of the lattice is preserved on average. An alternative formulation of the problem in terms of fluctuating dichotomous barriers between sites also seems possible [18]. Such models for dynamic random media are relevant for the description of several physiochemical processes like e.g. ligand diffusion in proteins [19] or proton migration in water [20].

On the other hand, if one goes back to the original picture of two dissimilar walkers  $A$  and  $B$ , the model may be regarded as a schematized starting point for describing the dynamics of exciton absorption in biological light-harvesting systems [21]. In photosynthetic cells, a photon is absorbed by the pigment molecules (e.g. chlorophyll) in the cell and may give rise to an excited energy state. The exciton hops by resonant energy transfer through a network or lattice of 200-500 pigment molecules (antenna system) and can be eventually trapped at a reaction center [22], which is usually considered to be immobile within the time scale for trapping (a few hundred picoseconds). The exciton energy is then used to trigger a series of redox processes in the chain of chemical reactions leading to the production of sugars and

carbohydrates. Thus, one of the time-limiting steps for the production of oxygen is precisely the absorption of the exciton by the trapping center. If we allow for a certain mobility of the reaction center (thereby generalizing Montroll's approach for exciton trapping), we can identify the latter with a slowly hopping walker, say the  $A$  walker, while the propagating exciton would play the role of the  $B$  walker. As long as the hopping rate of the  $A$  walker remains small, the situation may be identified with the almost purely asynchronous case (small  $p$ ); this is normally the case in *in vivo* light-harvesting systems. However, a modification of the physical properties of the antenna system so as to make exciton propagation slower might, at least in principle, lead to interesting antiresonance phenomena as observed in our model.

The paper is organized as follows. In Section 3.2, we define the two-walker system in detail and show how it can be recast into an equivalent one-walker system with absorbing sites. In Section 3.3, we report analytic work on the  $1d$  case and identify the principal differences between the purely asynchronous case ( $p = 0$ ), the purely synchronous case ( $p = 1$ ) and the mixed case ( $0 < p < 1$ ). These results are also supported by Monte Carlo simulations. In Section 3.4, similar results are found for the  $2d$  and the  $3d$  cases by means of simulations. In Section 3.5, the results are compared with the predictions of the continuum approximation valid for large lattices. Finally, Section 3.6 summarizes the main conclusions and discusses possible extensions.

### 3.2 Formulation of the problem: two-walker vs. one-walker picture

The starting point is a  $1d$  periodic lattice with  $N$  sites and discrete time dynamics (cf Fig. 3.1a). We place two walkers  $A$  and  $B$  on two distinct lattice sites and let them evolve at each time step as follows:

1. with probability  $p$ , both walkers hop simultaneously to randomly chosen nearest neighbor sites (*synchronous event*).
2. with probability  $1 - p$ , one of the walkers (no matter which one) remains at rest while the other performs a jump to a nearest neighbor site (*asynchronous event*).

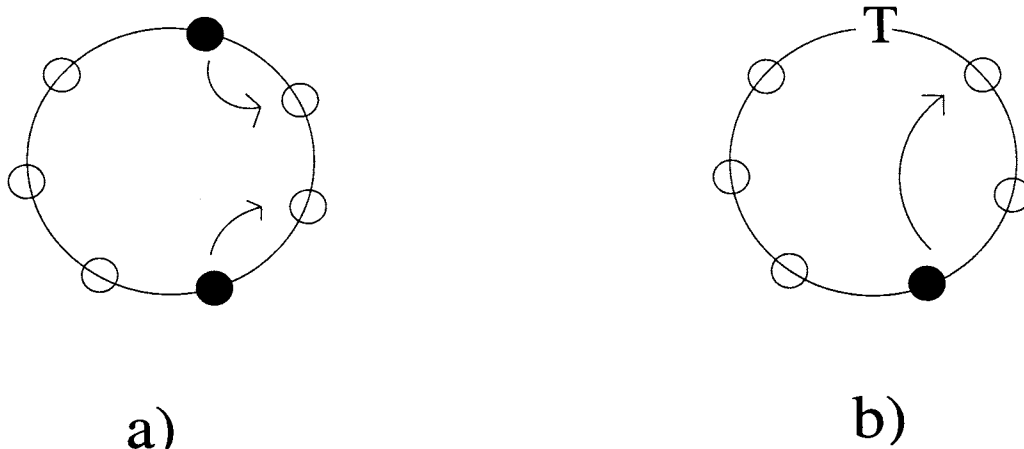


Figure 3.1 a) two-walker system on a seven-site periodic lattice (walkers represented by black circles). b) Equivalent one-walker system with trap. For convenience, the walker labels  $A$  and  $B$  in Fig. 3.1a have been left out. The arrows in Fig. 3.1a indicate that both walkers perform a synchronous step. In Fig. 1b this corresponds to a two-site jump of the walker.

The walkers are assumed to be unbiased, i.e., their jumps are symmetric. We additionally assume that their jump directions are completely uncorrelated. An encounter takes place when both walkers ‘land’ on the same site or attempt to exchange positions. Each encounter triggers instantaneously an irreversible reactive interaction, say the annihilation reaction  $A + B \rightarrow 0$ . The encounter time can thus be regarded as the characteristic reaction time governing the diffusion-controlled two-particle annihilation.

In principle, the mean encounter time can be computed for a single initial configuration of the walkers; in many practical situations, though, one has little knowledge about the initial conditions. We shall therefore give preference to a definition of the mean encounter time which contains an additional coarse graining over all possible initial configurations. In the sequel, we shall denote this quantity by  $\langle n \rangle$ . The smaller  $\langle n \rangle$ , the more efficient the reaction will be.

Note that, due to the translational invariance of the lattice, the physical distinguishability of the walkers is irrelevant for the computation of  $\langle n \rangle$ : in other words, it does not matter which of the walkers  $A$  or  $B$  hops more often, since  $\langle n \rangle$  depends only on the relative motion of both walkers, the latter being fully characterized by  $p$ . Therefore, we shall assume for simplicity and



without loss of generality that  $A$  and  $B$  are physically identical walkers and drop the labels  $A$  and  $B$ , as has been done in Fig. 3.1a.

For  $p = 0$ , only reactions through simultaneous site occupancy are possible. As far as  $\langle n \rangle$  is concerned, this case is equivalent to the one treated by Montroll [9]. However, if  $p > 0$ , reaction through position exchange becomes possible. This technical obstacle makes the analytical treatment of the problem more difficult.

A first step to circumvent this difficulty is to take advantage of the translational invariance of the lattice and reformulate the problem in terms of a single walker. To do so, we must switch over to a new co-moving reference frame in which one of the walkers remains stationary, thereby playing the role of a fixed perfect trap  $T$  (Fig. 3.1b). Clearly, an asynchronous event in the original two-walker system is equivalent to nearest neighbor hopping in the single-walker system, while a synchronous event results either in a walker's jump by two lattice sites (if both walkers hop in opposite directions in the original reference frame) or its remaining at rest (if they hop in the same direction). In this picture, reaction takes place any time the walker reaches or overreaches the trap  $T$ .

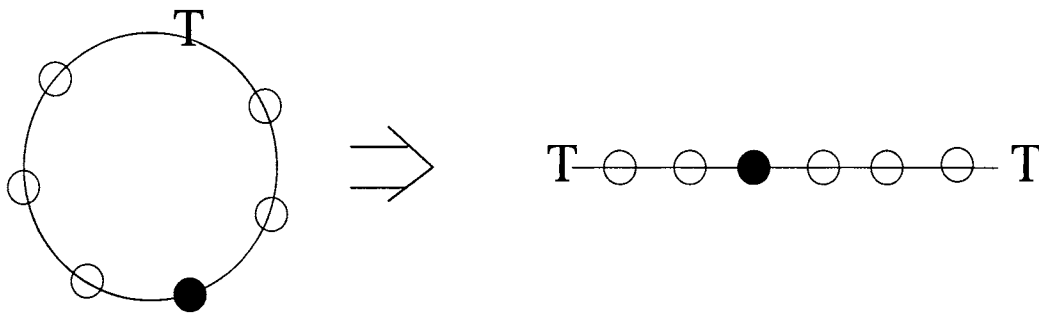


Figure 3.2 Lattice transformation for the one-walker system displayed in Fig. 3.1b.

We can now take advantage of the simple lattice geometry and the fact that the trap is perfect to unfold the  $N$ -site lattice into an equivalent one with  $N + 1$  sites and two perfect traps  $T$  sitting at each end site, as shown in Fig. 3.2 for  $N = 7$ . This transformation does not of course affect the characteristics of the walk; a walker jump in anticlockwise direction will be equivalent to a jump to the left by the same number of sites in the transformed lattice. Next,

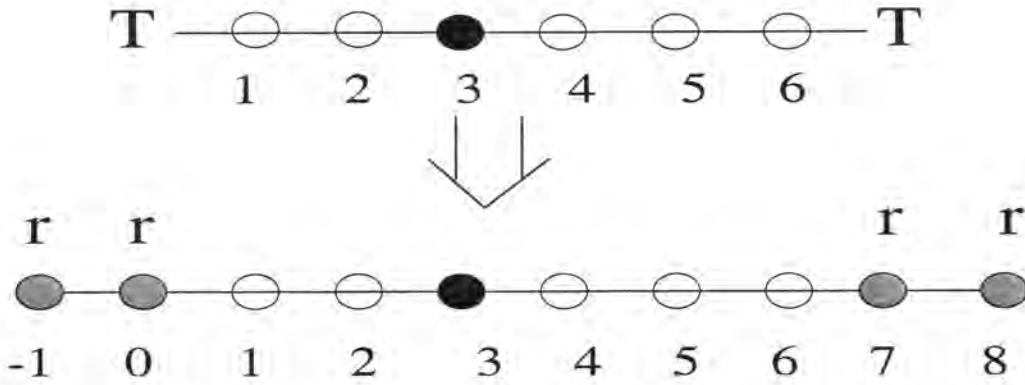


Figure 3.3 Replacement of the traps  $T$  at each end site of the transformed lattice by two absorbing sites  $r$ .

we replace each trap  $T$  by two (fictitious) reactive sites  $r$  (Fig. 3.3). The random walk will instantaneously terminate when the walker lands on any of these  $r$ -sites. We shall therefore occasionally call the  $r$ -sites “absorbing” in what follows.

Let us assign the coordinates 1 to  $N - 1$  to each of the non-absorbing sites, as shown in Fig. 3.3. Additionally, we term the  $r$ -sites at the left end  $-1$  and  $0$  and those at the right end  $N$  and  $N + 1$ . An attempt to overcome, say the left trap, triggered by a synchronous event will be equivalent to a jump from site 1 to site  $-1$ . In contrast, the walker’s landing on the trap can be realized either by an asynchronous event (jump from site 1 to site 0) or by a synchronous event (jump from site 2 to site 0). If the dynamics is purely asynchronous, only one  $r$ -site at each end will be needed, since jumps by two sites are not possible in this case. Thus, events involving position exchange can be dealt with by going over to a one-walker picture and introducing fictitious absorbing sites. The mean duration of the walk averaged over the initial positions  $1, \dots, N - 1$  of the walker plays the role of  $\langle n \rangle$  in the original two-walker system.

A standard approach for the calculation of  $\langle n \rangle$  is to formulate the problem for the restricted walk between the absorbing sites in terms of a conditional first passage problem for an unrestricted walk on an infinite  $1d$  lattice [23]. The starting point is the Markovian master equation

$$P_{n+1}(j) = \frac{p}{4} [P_n(j-2) + 2P_n(j) + P_n(j+2)] + \frac{1-p}{2} [P_n(j-1) + P_n(j+1)], \quad (3.1)$$

where  $P_n(j)$  is the probability to find the walker at a given site  $j$  in the infinite lattice after  $n$  time steps. The first term on the right hand side of eq. (3.1) is the contribution due to the synchronous events, by which the walker either remains at rest or it moves two lattice sites either to the left or to the right. The second term describes jumps by one lattice site as a consequence of asynchronous events. The mean time to absorption  $\langle n \rangle$  can now be viewed as a first-passage time and computed via a generating function approach [23]. Specifically,  $\langle n \rangle$  can be expressed in terms of the generating function for the probability of the walker arriving for the first time at a given  $r$ -site after a given number of steps without having been previously in neither of the other three  $r$ -sites. Unfortunately, the resulting expressions for  $\langle n \rangle$  are not very transparent and their analytical dependence on  $N$  and  $p$  is not easy to determine.

Another possibility is to make use of the single step probabilities appearing as coefficients in the right hand side of eq. (3.1) to compute the transition probabilities between the states of the underlying absorbing Markov chain. In this approach,  $\langle n \rangle$  can be related to the row sums over the elements of the fundamental matrix for the transition to the absorbing state or, alternatively, to its smallest eigenvalue [24]. The disadvantage of this method is that it requires the inversion of increasingly large matrices as  $N$  becomes large.

Finally, the method we shall further develop here exploits the analogy of our random walk problem with the classical ruin problem studied by Feller [5]. Even though this approach has the disadvantage of being difficult to generalize to higher dimensions, it provides an elegant solution for the  $1d$  problem.

### 3.3 Connection with ruin problem and analytical solution

We first recall briefly the classical gambler's ruin problem. Consider a single walker (in our setting, this would correspond to the limit  $p=0$ ), whose position  $z$  is viewed as the capital of a gambler playing against an adversary whose capital is  $N - z$ . At each time step, a trial is made, as a result of which the gambler wins or loses one euro. Thus, the gambler's winning corresponds to a nearest neighbor jump of the walker to the right, while losing the trial corresponds to a jump to the left. The game goes on until the gambler's capital is reduced

to zero or increases to  $N$  (absorption of the walker at sites 0 or  $N$ ). One is interested in the mean duration of the game  $\langle n \rangle_z$  when the gambler starts with a given capital  $z$ . This quantity can be shown to be finite as long as  $N < \infty$  and obeys the following difference equation [5]:

$$\langle n \rangle_z = \frac{1}{2} \langle n \rangle_{z+1} + \frac{1}{2} \langle n \rangle_{z-1} + 1, \quad 0 < z < N \quad (3.2)$$

with the boundary conditions

$$\langle n \rangle_0 = 0 \quad \text{and} \quad \langle n \rangle_N = 0. \quad (3.3)$$

Eq. (3.2) states that the walker has no memory of where it has been at earlier time steps; if it is initially at site  $z$ , it will either jump to site  $z+1$  or to site  $z-1$  with probability  $1/2$ . Once at any of these sites, the walker will continue his walk without remembering its previous position  $z$ . It is as though the walker started a new walk from  $z+1$  or  $z-1$  with equal probability, except that the expected value of the mean time to absorption must be increased by one unit [25]. The boundary conditions (3.3) reflect the fact that, if the walker is initially placed at a  $r$ -site, it is immediately absorbed. In the original two-walker system, this is equivalent to placing both walkers at the same site.

Eqs. (3.2)-(3.3) can be solved by standard methods, e.g. by writing the general solution as the sum of the general solution of the corresponding homogeneous equation plus a particular solution [26]. One obtains in this way

$$\langle n \rangle_z = z(N-z), \quad (3.4)$$

and

$$\langle n \rangle = \frac{1}{N} \sum_{z=1}^{N-1} \langle n \rangle_z = \frac{N(N+1)}{6}. \quad (3.5)$$

The opposite limit of the above ( $p = 1$ ), corresponding in our setting to a purely synchronous motion of *two* walkers, is somewhat less standard. In this case, only jumps by zero or two lattice sites may occur. Depending on its initial position, the walker may land on any of the four  $r$ -sites depicted in Fig. 3.3. Therefore, two additional boundary conditions for the absorbing sites  $-1$  and  $N+1$  are needed.

In the gambler's jargon, a jump by two sites means doubling the stake of each trial, i.e., the player wins or loses two euros with probability  $1/4$ . Besides, a tie occurs with probability  $1/2$  (no jump). The game terminates when either the player or his adversary reaches or overreaches a capital of  $N$  euros. Now, the difference equation for the duration of the game is a fourth-order one:

$$\langle n \rangle_z = \frac{1}{4} \langle n \rangle_{z+2} + \frac{1}{2} \langle n \rangle_z + \frac{1}{4} \langle n \rangle_{z-2} + 1, \quad 0 < z < N. \quad (3.6)$$

The solution of this equation requires four boundary conditions, namely

$$\langle n \rangle_{-1} = 0, \quad \langle n \rangle_0 = 0, \quad \langle n \rangle_N = 0 \quad \text{and} \quad \langle n \rangle_{N+1} = 0. \quad (3.7)$$

A particular solution of (3.6) is given by  $-\frac{1}{2}z^2$ . The characteristic equation of the homogeneous equation has two double roots  $\lambda_{1,2} = \pm 1$ . Therefore, the full inhomogeneous solution reads

$$\langle n \rangle_z = -\frac{1}{2}z^2 + c_1 + c_2z + (c_3 + c_4z)(-1)^z, \quad (3.8)$$

Substituting into eq. (3.6) one obtains a system of equations for  $c_1$  to  $c_4$  whose solution yields

$$\begin{aligned} \langle n \rangle_z &= (z(N-1-z) + N)/2 && \text{for } z \text{ odd, } N \text{ odd,} \\ &= z(N+1-z)/2 && \text{for } z \text{ even, } N \text{ odd,} \\ &= (z(N-z) + (N+1))/2 && \text{for } z \text{ odd, } N \text{ even,} \\ &= z(N-z)/2 && \text{for } z \text{ even, } N \text{ even.} \end{aligned} \quad (3.9)$$

The spatially averaged time to absorption  $\langle n \rangle$  is again easily computed. One obtains

$$\begin{aligned} \langle n \rangle &= N(N+1)(N+2)/12(N-1) && \text{for } N \text{ even,} \\ &= (N+1)(N+3)/12 && \text{for } N \text{ odd.} \end{aligned} \quad (3.10)$$

For notational convenience, let us rename the value of  $\langle n \rangle$  obtained from eqs. (3.10) as  $\langle n \rangle^{(1)}$ , and the corresponding result of Montroll for the one-walker problem (eq. (3.5)) as  $\langle n \rangle^{(0)}$ . A comparison between  $\langle n \rangle^{(0)}$  and  $\langle n \rangle^{(1)}$  is shown in Fig. 3.4. As expected, the synchronous case becomes more efficient as soon as the lattice gets sufficiently large ( $N \geq 5$ ). In the limit of a very large lattice, it is asymptotically twice as efficient as the asynchronous case [see Fig. 3.5)].

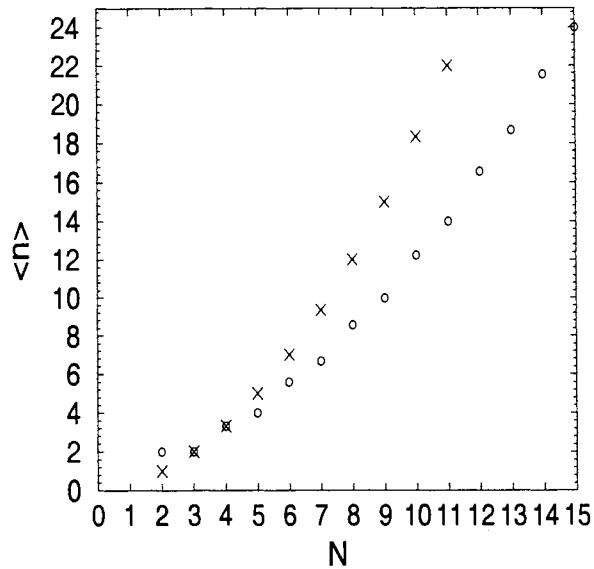


Figure 3.4 Mean encounter time as a function of the lattice size for the purely synchronous case  $\langle n \rangle = \langle n \rangle^{(1)}$  (circles) and the purely asynchronous case  $\langle n \rangle = \langle n \rangle^{(0)}$  (crosses).

It is also worth comparing the  $z$ -distribution of the encounter time for the case  $p = 1$  (eq. (3.9)), with the earlier known result for  $p = 0$  (eq. (3.4)). For odd  $N$ , the spatial profile in  $z$  displays some qualitative similarities in both cases (cf. Figs. 3.6a and 3.6b). The highest value of  $\langle n \rangle_z$  is attained at those sites located at maximum distance  $d_z$  from the closest absorbing site. For  $p = 0$ , the encounter time always increases with increasing  $d_z$ , and it becomes maximum when  $z = (N \pm 1)/2$ . In contrast, the behavior is no longer strictly monotonic for  $p = 1$ , since  $\langle n \rangle_z$  either increases *or* remains constant as  $d_z$  becomes larger, giving rise to a “staircase” profile for high enough values of  $N$  (Fig. 3.6b).

For even lattices, there are more marked differences between the cases  $p = 0$  and  $p = 1$ . For  $p = 0$ , the discrete spatial profile resembles an inverted parabola like in the odd lattice case, the maximum now being located at  $z = N/2$ . However, if  $p = 1$ , one observes a series of alternating valleys and peaks in the distribution (cf Figs. 3.7a and 3.7b). There are two subcases here: if  $N$  is divisible by 4, the highest values of  $\langle n \rangle_z$  are attained for  $z = (N \pm 2)/2$  (Fig. 3.7a). Otherwise, the maximum value corresponds again to  $z = N/2$  (Fig. 3.7b).

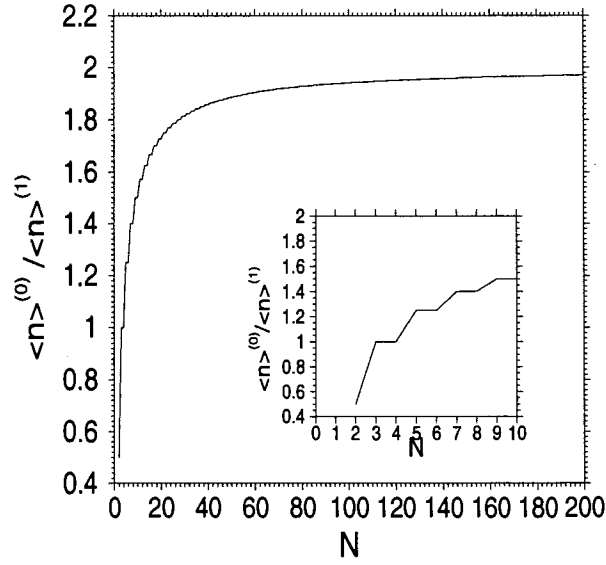


Figure 3.5 Ratio  $\langle n \rangle^{(0)} / \langle n \rangle^{(1)}$  as a function of  $N$ . Note that the value of the ratio is the same for two consecutive odd and even values of  $N$ . The inset displays the behaviour for small  $N$ .

Note that for  $p = 0$  and even  $N$  the time to absorption when the walker is started at sites 1 or  $N - 1$  is smaller than in the purely synchronous case. An intuitive argument points to the fact that, in the former case, the walker is absorbed one out of two times after the first time step, while absorption takes place only one out of four times if  $p = 1$ . However, this argument should be taken with care, since it fails for odd  $N$ . Besides, as we shall see later on, the minimum of  $\langle n \rangle_1 = \langle n \rangle_{N-1}$  corresponds to a process with  $p > 0$ .

We finally turn to the general case of a mixed walk. Assume that a given event is synchronous with probability  $0 < p < 1$  and asynchronous with probability  $1 - p$ . The difference equation for  $\langle n \rangle_z$  now reads:

$$\langle n \rangle_z = \frac{p}{4} \langle n \rangle_{z+2} + \frac{1-p}{2} \langle n \rangle_{z+1} + \frac{p}{2} \langle n \rangle_z + \frac{1-p}{2} \langle n \rangle_{z-1} + \frac{p}{4} \langle n \rangle_{z-2} + 1, \quad 0 < z < N. \quad (3.11)$$

The boundary conditions are again given by (3.7). A particular solution of eq. (3.11) is given by  $-z^2/(1+p)$ . The roots of the underlying characteristic equation are

$$\lambda_{1,2} = 1, \quad \lambda_{3,4} = \frac{-1 \pm \sqrt{1-p^2}}{p}. \quad (3.12)$$

$N$	$\langle n \rangle$
2	$2/(2-p)$
3	$2$
4	$(10/3) \frac{3p-4}{p^2+2p-4}$
5	$4(2p-5)/(p^2-4)$
6	$(28/5)(p^2-10p+10)/(p^3-4p^2-4p+8)$
7	$(4/3)(p^2+8p-14)/(p^2-2)$
8	$(12/7)(13p^3+6p^2-126p+112)/((p-2)(p^3+6p^2-8))$
9	$10(2p^3-5p^2-16p+24)/((p^2+2p-4)(p^2-2p-4))$
10	$(22/9)(7p^4-76p^3+16p^2+288p-240)/(p^5-6p^4-12p^3+32p^2+16p-32)$

Table 3.1 Analytic expressions for  $\langle n \rangle$ .

The full solution reads

$$\langle n \rangle_z = -z^2/(1+p) + c_1 + c_2 z + c_3 \lambda_3^z + c_4 \lambda_4^z, \quad (3.13)$$

where the constants  $c_1 - c_4$  are now given by the linear system

$$-\frac{1}{1+p} + c_1 - c_2 + \lambda_3^{-1} c_3 + \lambda_4^{-1} c_4 = 0, \quad (3.14a)$$

$$c_1 + c_3 + c_4 = 0, \quad (3.14b)$$

$$-\frac{N^2}{1+p} + c_1 + N c_2 + \lambda_3^N c_3 + \lambda_4^N c_4 = 0, \quad (3.14c)$$

$$-\frac{(N+1)^2}{1+p} + c_1 + (N+1) c_2 + \lambda_3^{N+1} c_3 + \lambda_4^{N+1} c_4 = 0. \quad (3.14d)$$

We prefer to omit the rather lengthy analytic form of the coefficients  $c_1 - c_4$ . From the above equations,  $\langle n \rangle_z$  and  $\langle n \rangle$  can be explicitly computed. For  $\langle n \rangle$  one has an expression of the form

$$\begin{aligned} \langle n \rangle &= -\frac{N(2N-1)}{6(1+p)} + c_1(N,p) + \frac{N c_2(N,p)}{2} \\ &\quad + \frac{1}{N-1} (c_3(N,p) [\lambda_3(p)]^{N-1} + c_4(N,p) [\lambda_4(p)]^{N-1}). \end{aligned} \quad (3.15)$$

Table 3.1 displays the analytical expressions of  $\langle n \rangle$  as a function of  $p$  for increasing values of  $N$ . These are rational functions of  $p$  whose complexity increases with  $N$ . For  $N \geq 4$  and small  $p$ , one can obtain a first-order approximation to the exact solution by Taylor-expanding eq. (3.15):

$$\langle n \rangle = \langle n \rangle^{(0)} \left[ 1 + \frac{N-3}{N} p + \mathcal{O}(p^2) \right]. \quad (3.16)$$



Figs. 3.8a and 3.8b contain several numerical plots of  $\langle n \rangle$ , as a function of  $p$  for different values of  $N$ . For  $N = 2$ , the purely asynchronous case is more effective than the purely synchronous case<sup>6</sup>. As synchronicity is turned on, a monotonic increase of  $\langle n \rangle$  as a function of  $p$  is observed. For  $N = 3$ ,  $\langle n \rangle$  does not depend on  $p$ . At each individual time step, the probability of reaction is always  $1/2$ , regardless of whether both walkers hop or only one of them. In a sense, the cases  $N = 2$  and  $N = 3$  are non-generic, since they only involve a single symmetry-distinct initial condition. For  $N \geq 4$ , a new parity effect appears: if  $N$  is even, the most effective process is observed for an intermediate value of  $p$  associated to a minimum of the function  $\langle n \rangle$  in the physically acceptable  $p$ -interval  $[0, 1]$ ; in contrast, for odd lattices,  $\langle n \rangle$  is a monotonically decreasing function of  $p$ , i.e., the most effective process is always the purely synchronous one. For  $N = 4$ , any intermediate value of  $p$  makes hopping more effective than in both limiting cases, and a minimum of  $\langle n \rangle$  is obtained for  $p_{min} = 2/3$ . For higher, even values of  $N$ , the minimum is rapidly shifted to the right ( $p_{min} \approx 0.86$  for  $N = 6$ ) and the  $p$ -interval for which processes are more efficient than the purely synchronous case shrinks dramatically. For large  $N$ ,  $p_{min}$  gets arbitrarily close to 1 (see Table 3.2).

$N$	$p_{min}$
2	0.0000
4	0.6667
6	0.8596
8	0.9204
10	0.9483
12	0.9636
14	0.9729
16	0.9791

Table 3.2 Values of  $p_{min}$  with 4-digit accuracy.

A series of Monte Carlo simulations for the periodic two-walker system has been carried out to confirm our analytic results based on the one-walker description. For two different lattice sizes, namely  $N = 7$  and  $N = 8$ , we have performed a series of statistical runs to compute  $\langle n \rangle$ , each run thereby comprising a whole set of symmetric-distinct nonreactive configurations. Due

<sup>6</sup>Obviously, the purely asynchronous case has a maximum efficiency in this case, since the walker is always trapped after the first step.

to the large variability  $\langle n^2 \rangle - \langle n \rangle^2$  characteristic of first-passage problems, a relatively high number of runs was needed ( $10^6$ ) to obtain an accurate value for  $\langle n \rangle$ . The  $\langle n \rangle$ -values obtained from simulations (with an accuracy of three significant digits) are listed in Tables 3.3 and 3.4 for the cases  $N = 7$  and  $N = 8$ , respectively. The agreement with the analytical predictions is good, the maximum observed deviation is off the theoretical value by about 1% only.

$p$	$\langle n \rangle^{sim}$	$\langle n \rangle^{theo}$
0.2	8.410	8.408163
0.5	7.430	7.428571
0.8	6.826	6.823529
1	6.667	6.666667

Table 3.3 Theoretical vs. simulation value of  $\langle n \rangle$  for  $N = 7$ .

$p$	$\langle n \rangle^{sim}$	$\langle n \rangle^{theo}$
0.2	10.709	10.706177
0.5	9.345	9.344538
0.8	8.495	8.496241
1	8.572	8.571429

Table 3.4 Theoretical vs. simulation value of  $\langle n \rangle$  for  $N = 8$ .

In order to obtain additional insight in the even-odd transition mechanism, we have studied qualitatively  $\langle n \rangle_z$  as a function of  $p$  and  $N$  for each single initial position  $z$  of the walker. Let us characterize each site  $z$  by its distance  $d_z = \min(z, N - z)$  to the closest  $r$ -site. For not too large values of  $p$ , the behavior of the encounter time is roughly the same for all  $z$  values regardless of the parity of  $N$ , i.e., a decrease of the encounter time is observed (Figs. 3.9a and 3.9b). However, the qualitative  $p$ -dependence of  $\langle n \rangle_z$  in the large  $p$  limit becomes different for initial positions with even or odd values of  $d_z$ : for even values of  $N$  and initial positions with odd  $d_z$ ,  $\langle n \rangle_z$  begins to increase sharply, as a result of which a minimum of the curve is observed (cf Fig. 3.9a). Even though the contribution to the global efficiency  $\langle n \rangle$  arising from the  $(N/2) - 1$  sites with even  $d_z$  decreases strongly in this regime, this effect is overcome by the increase of the contribution yielded by the  $N/2$  sites with odd  $d_z$ , thus giving rise to a net increase in  $\langle n \rangle$ . In contrast, the sensitivity to the initial condition is less systematic and less

important for odd values of  $N$  (Fig. 3.9b): again, a monotonic decrease is observed for even  $d_z$ . Even though minima are still observed for  $d_z = 1$ , for all other odd values of  $d_z$ , they are either absent<sup>7</sup> or very flat (see curve for  $d_z = 3$  in Fig. 3.9b).

### 3.4 Monte Carlo results in two and three dimensions

To complement the analytic  $1d$  results for the dependence of  $\langle n \rangle$  on the value of the parameter  $p$ , we have also investigated how  $\langle n \rangle$  depends on  $p$  for dimensions  $2d$  and  $3d$  using Monte Carlo simulations. Figures 3.10 and 3.11 show the dependence of  $\langle n \rangle$  with respect to  $p$ . As shown above for  $1d$ , there is distinctively different behavior based on whether  $N$  is even or odd. In higher dimensions this even-odd effect becomes much more pronounced. It is clear that when  $N$  is an even number, the maximal efficiency is attained at some intermediate value between 0 and 1. Also, one notices that for the  $6 \times 6$  square lattice and for all  $3d$  even lattices which we studied  $\langle n \rangle^{(0)} < \langle n \rangle^{(1)}$ . This is a surprising result which we do not see in the  $1d$  case for lattices with  $N > 4$ . This suggests the existence of a crossover effect in the large size limit when switching from  $2d$  to  $3d$  lattices, implying that in the former case the two simultaneously moving walkers are more effective than two asynchronous walkers, while in  $3d$  the opposite holds. As in the  $1d$  case, the value of  $p_{min}$  in  $2d$  and  $3d$  tends toward 1 in the limit of large lattice size, but it is interesting to note that in the largest  $3d$  lattice which we studied ( $N = 1000$ ), the difference between  $p = 0.999$  and  $p = 1$  is  $\sim 600$ , which is about 30% of  $\langle n \rangle^{(1)}$  in that case. This shows that for even lattices, a minute amount of asynchronicity allows for a much greater efficiency. Similar arguments to those given above for  $1d$  exist for in  $2d$  and  $3d$  when attempting to determine why such even-odd behavior arises, and further analysis of this striking behavior is given in Ref. [27].

### 3.5 Comparison with continuum approximation

It is instructive to compare the above results in  $1d$  with the continuum approximation valid for large  $N$ . To do so, consider the one-walker system with absorbing sites and a fixed

---

<sup>7</sup>This is e.g. the case for  $N = 7$  and  $d_z = 3$  (not shown here).

lattice length  $L = N\Delta x$ , where  $\Delta x$  is the intersite distance (lattice constant). According to this definition,  $L$  is the distance between the inmost  $r$ -sites. The walker's distance to site 0 is  $x = z\Delta x$ . We perform the continuum limit by letting  $\Delta x$  and  $\Delta t$  simultaneously go to zero under the additional requirement that the diffusive combination  $(\Delta x)^2/\Delta t$  tend to a finite constant. Since  $L$  is fixed, this implies that one lets the number of sites  $N$  go to infinity while the spatial and temporal resolutions  $\Delta x$  and  $\Delta t$  are scaled as  $1/N$  and  $1/N^2$ , respectively. Let us next replace  $\langle n \rangle_z$  by a function  $\langle n \rangle_x$  varying smoothly in the space interval  $[0, L]$ . The mean elapsed time  $\langle t \rangle_x$  to absorption will then simply be the mean number of steps  $\langle n \rangle_x$  times the time unit  $\Delta t$ . From eq. (3.11), we have:

$$\frac{p}{4} [\langle t \rangle_{x+2\Delta x} - 2\langle t \rangle_x + \langle t \rangle_{x-2\Delta x}] + \frac{1-p}{2} [\langle t \rangle_{x+\Delta x} - 2\langle t \rangle_x + \langle t \rangle_{x-\Delta x}] + \Delta t = 0 \quad (3.17)$$

with the boundary conditions <sup>8</sup>

$$\langle t \rangle_{-\Delta x} = \langle t \rangle_x = \langle t \rangle_L = \langle t \rangle_{L+\Delta x} = 0. \quad (3.18)$$

We now divide eq. (3.17) by  $\Delta t$  and expand the expressions in the brackets in  $\Delta x$ . Taking the diffusive limit in the resulting equation yields

$$D \frac{d^2 \langle t \rangle_x}{dx^2} = -1, \quad (3.19)$$

where the relative diffusion coefficient  $D$  is given by

$$D = (1+p) \lim_{\Delta x, \Delta t \rightarrow 0} \frac{(\Delta x)^2}{\Delta t} = (1+p) D^{(0)}. \quad (3.20)$$

In the rightmost equation,  $D^{(0)}$  is the value of the diffusion coefficient for  $p = 0$ . For  $p > 0$ ,  $D^{(0)}$  is increased by the prefactor  $1+p$ , i.e., the variance of the single-step probabilities of the random walk. In this limit, the four boundary conditions (3.18) coalesce into two distinct ones, namely  $\langle t \rangle_0 = 0$  and  $\langle t \rangle_L = 0$ . The solution of (3.19) which fulfils these boundary conditions is

$$\langle t \rangle_x = \frac{x(L-x)}{2D}. \quad (3.21)$$

The spatially averaged reaction time  $\langle t \rangle$  is obtained by integrating over  $x$ :

$$\langle t \rangle = \frac{1}{L} \int_0^L \langle t \rangle_x dx = \frac{L^2}{12D}. \quad (3.22)$$

---

<sup>8</sup>In the case  $p = 0$ , one only has two boundary conditions, namely  $\langle t \rangle_0 = \langle t \rangle_L = 0$ .

As expected,  $\langle t \rangle$  is proportional to the squared lattice length and inversely proportional to the relative diffusion coefficient  $D$ . For the special cases  $p = 0$  and  $p = 1$ , this result is recovered by directly taking the diffusive limit in the discrete solutions (3.5) and (3.10). The relation (3.22) leads to the asymptotic law

$$\frac{\langle t \rangle^{(0)}}{\langle t \rangle} = \lim_{N \rightarrow \infty} \frac{\langle n \rangle^{(0)}}{\langle n \rangle} = 1 + p, \quad (3.23)$$

where  $\langle t \rangle^{(0)} = L^2/(12D^{(0)})$  and  $\langle n \rangle$  is given by eq. (3.15). Eq. (3.23) shows that in the continuum limit, the efficiency of the reaction increases linearly with  $p$ . The continuum approximation applies for sufficiently large  $N$ , namely when the typical displacement of the walker  $\Delta l \equiv \sqrt{1+p} \Delta x$  at each time step is small compared to the lattice length  $N\Delta x$ . If this condition is not fulfilled, the approximation gets significantly worse at large values of  $p$  (cf Fig. 3.12).

A generalization of (3.19) for higher order moments  $\langle t^j \rangle_x$  can be obtained by writing down the difference equations for the discrete quantities  $\langle n^j \rangle_z$  and taking the diffusive limit thereof. One then gets the coupled set of equations

$$D \frac{d^2 \langle t^{j+1} \rangle_x}{dx^2} = -(j+1) \langle t^j \rangle_x, \quad (3.24)$$

Eqs. (3.24), not to be further dealt with here, are well known from the theory of first-passage problems, where they are usually obtained from the adjoint Fokker-Planck equation for the underlying diffusion process [23, 28]. Again, deviations from the dynamics dictated by (3.24) are expected for small lattices.

### 3.6 Conclusions and outlook

We have seen that the  $1d$  problem of computing the mean reaction time between two diffusing co-reactants can be reduced to a trapping problem for a single walker. The latter can be viewed as a generalized ruin problem, the duration of the game plays thereby the role of the mean time to absorption.

In the diffusive limit, equivalent to the limit  $N \rightarrow \infty$  if the lattice length  $L$  is held fixed, the reaction efficiency increases linearly with  $p$ , but important deviations are observed for not

too large values of  $N$ . Beyond the crossover size  $N = 4$ , a new parity effect is observed. For odd values of  $N$ , the reaction time still increases monotonically (but no longer linearly) with  $p$ , while for even values of  $N$ , the efficiency is optimized for an intermediate value  $p_{min} < 1$ . In higher dimensions, this parity effect is even more pronounced, i.e. for even lattices there is a drastic increase in efficiency when a tiny amount of synchronicity is introduced. In contrast to the  $1d$  case, the effect is enhanced with increasing  $N$ .

Let us briefly comment on the  $1d$  results from the perspective of the ruin problem. Assume that one of the gamblers is successively given an starting capital of  $1, 2, \dots, N - 1$  euros at each round, while his adversary gets  $N - 1, N - 2, \dots, 1$  euros. Let us further suppose that the gamblers can choose between two kinds of trials: the stake for the first one is one euro and there is no tie. In the second trial, either nobody wins or one of the gamblers wins two euros. According to our results, for an odd capital  $N$ , the gamblers minimize the average playing time if they always make a two-euro bet. However, if  $N$  is even, they should make a small amount of one-euro bets in order to finish the round as soon as possible.

Our work can be extended in many different ways. Perhaps the most straightforward one is the detailed characterization of the whole distribution  $P(n)$  in terms of  $p$  and  $N$ .

A generalization of results such as equation (3.23) to higher dimensional integral and fractal lattices is also of interest, since it may further clarify the role of dimensionality and the lattice coordination number. According to our results, in one-dimension two synchronously moving walkers are asymptotically twice as efficient as when they hop one after the other. In a 2d square planar lattice, Kozak *et al.* have shown that the purely synchronous case is  $\sqrt{2}$  times more efficient than the purely asynchronous one in the large  $N$  limit for odd lattices [10]. The question is whether or not the relative efficiency of both processes in lattices with fractal dimension  $1 < d_f < 2$  lies between 2 and  $\sqrt{2}$ . Preliminary calculations on a Sierpinski gasket (with fractal dimension  $d_f = 1.585$ ) seem to indicate an asymptotic relative efficiency higher than 2 in this case, despite the fact that the lattice has (up to the three vertex sites) the same coordination number as a 2d square planar lattice [27]. The reason for this may be the important role played by the specific form of the lattice boundaries, even in the limit of a

large lattice. This may motivate the study of boundary conditions other than periodic ones for the two-walker system. However, the analytical treatment of this case is considerably harder, at least in the framework of the method of difference equations, since the lattice is no longer translationally invariant.

As a further extension of our work, one can also consider more complex reactive schemes [29] involving more than two walkers to study the combined effect of synchronicity and many-body effects.

### **Acknowledgements**

We are indebted to K. Karamanos, M. Plapp, A. Provata and F. Vikas for fruitful discussions. The authors gratefully acknowledge financial support from the Université Libre de Bruxelles. This work is also supported by a NATO Cooperative linkage grant PST.CLG.977780 and by the European Space Agency under contract number 90043. One of us (JLB) acknowledges support from the Arthur P. Hellwig Award.

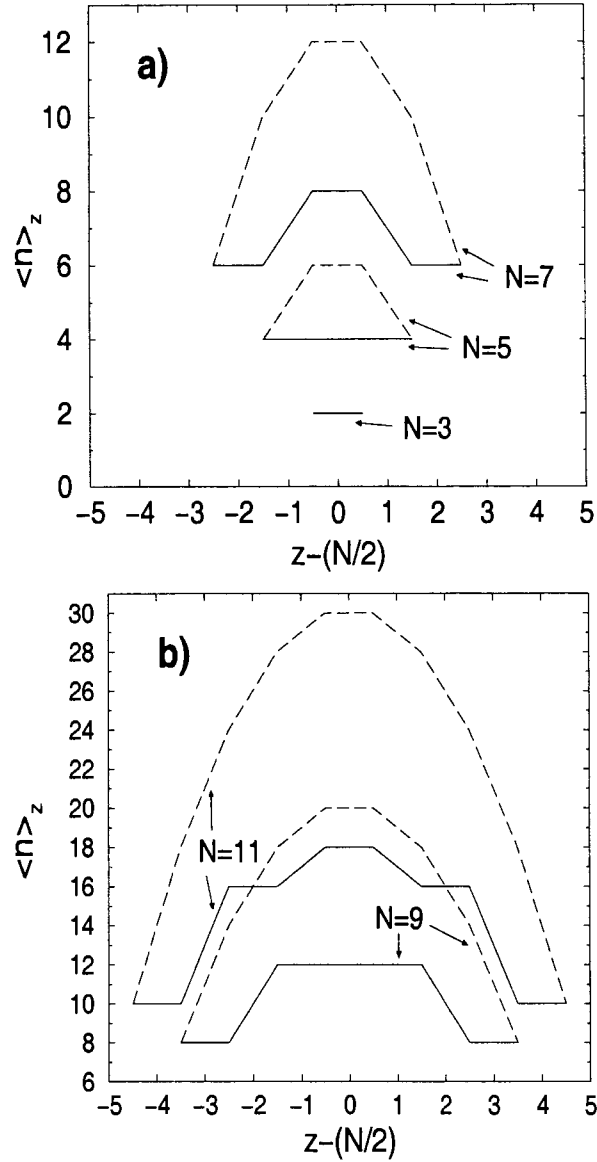


Figure 3.6  $z$ -distribution of the encounter time in the cases  $p = 0$  (dashed lines) and  $p = 1$  (continuous lines) for a)  $N = 3, 5, 7$  and b)  $N = 9, 11$ . For  $N = 3$  both cases display the same flat distribution.



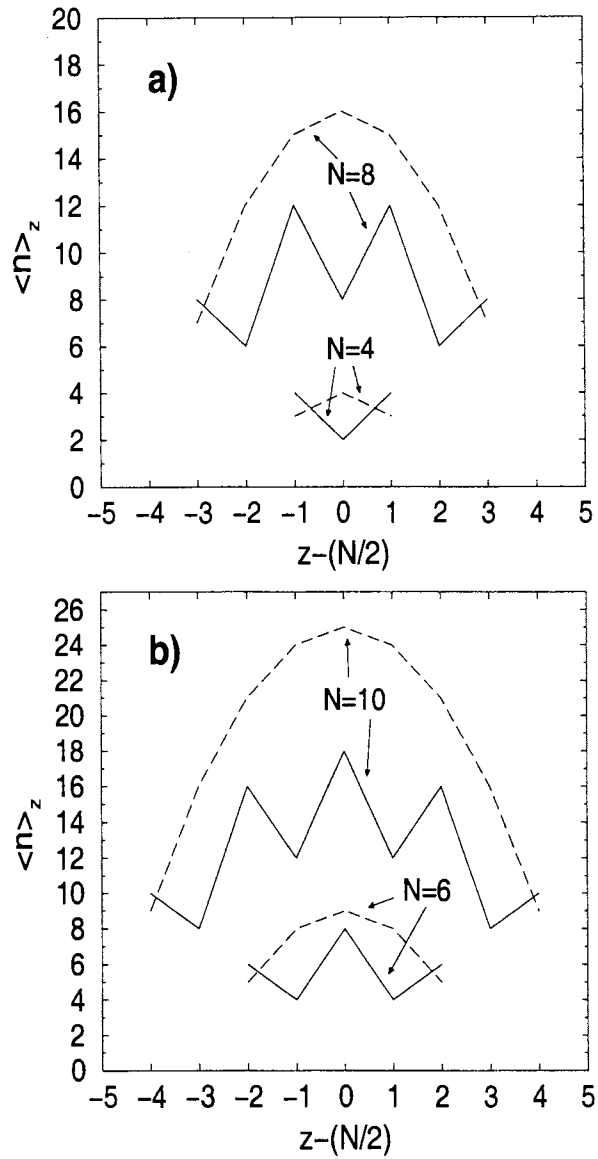


Figure 3.7  $z$ -distribution of the encounter time for  $p = 0$  (dashed lines) and  $p = 1$  (continuous lines) for a)  $N = 6, 10$  and b)  $N = 4, 8$ .

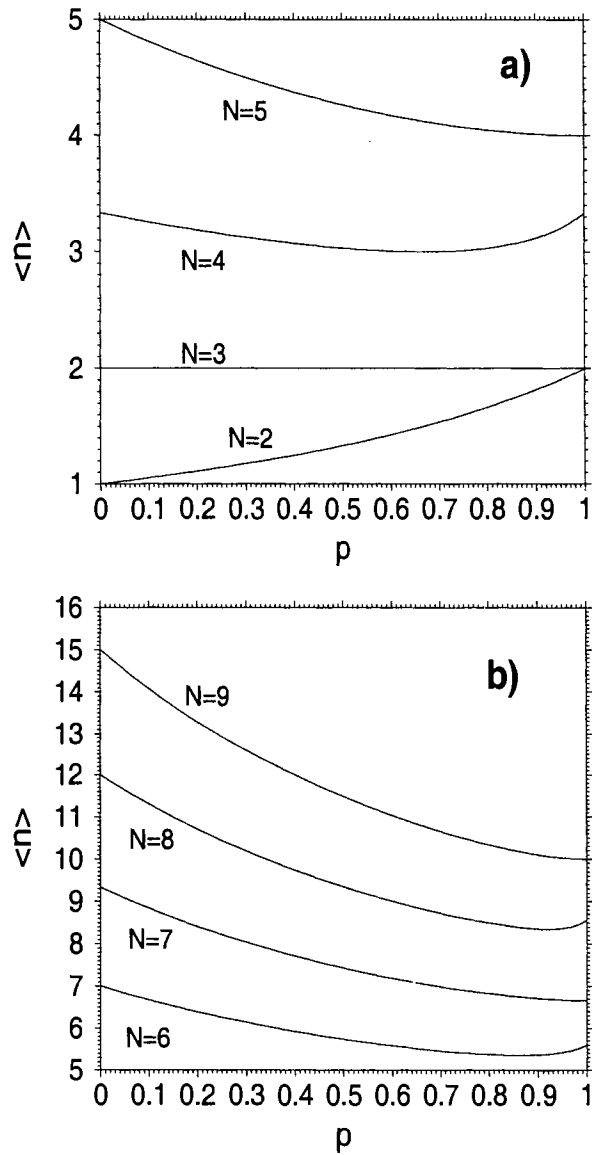


Figure 3.8 Mean encounter time as a function of  $p$  for a)  $N = 2, \dots, 5$  and b)  $N = 6, \dots, 9$ .

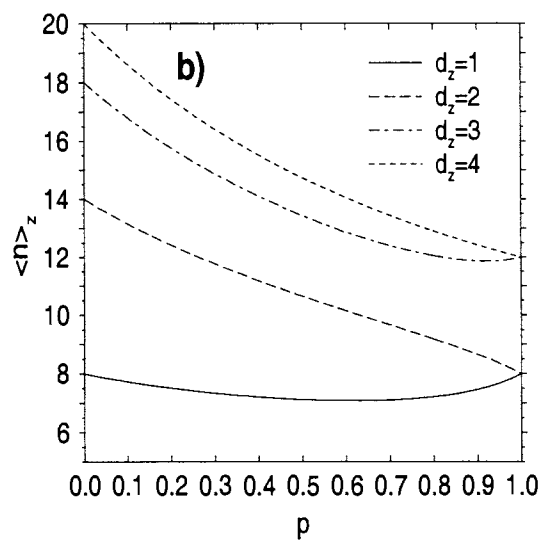
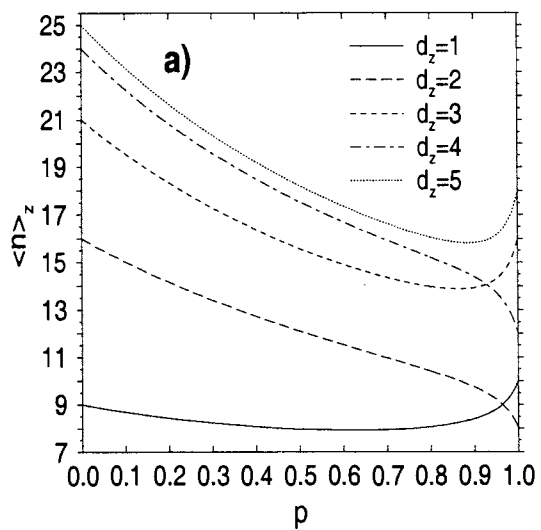


Figure 3.9 a)  $p$ -dependence of  $\langle n \rangle_z$  for all possible values of  $d_z$  on a lattice with a) 10 sites b) 9 sites.

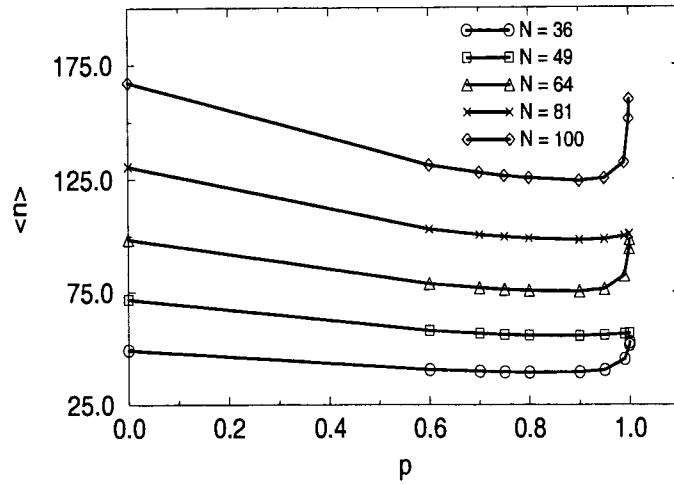


Figure 3.10 Mean encounter time as a function of  $p$  for two walkers on a  $2d$  square planar lattice with periodic boundary conditions.

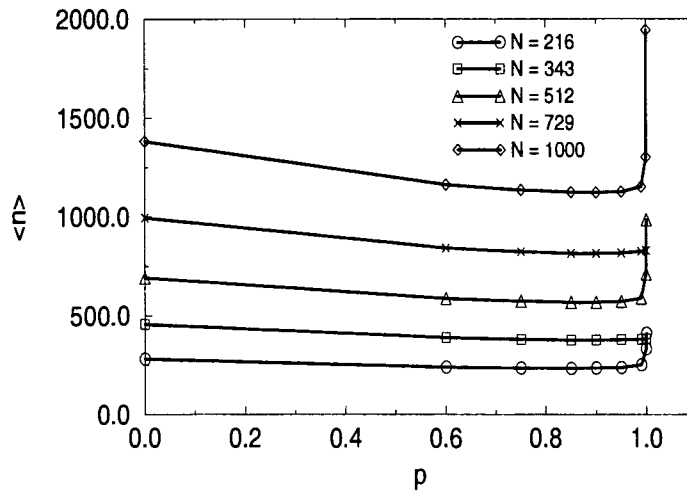


Figure 3.11 Mean encounter time as a function of  $p$  for two walkers on a  $3d$  cubic lattice with periodic boundary conditions.

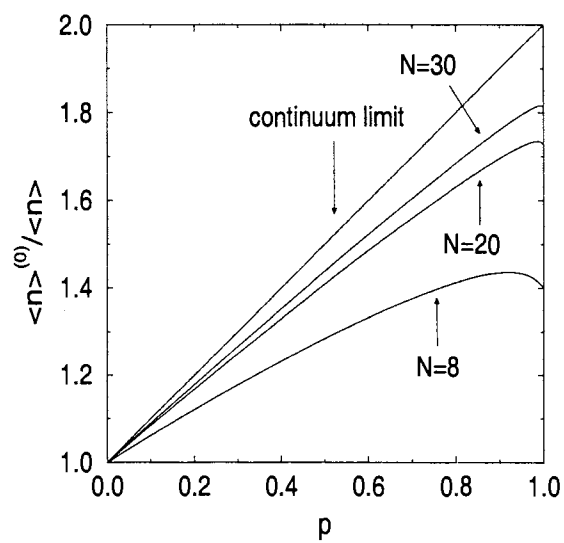


Figure 3.12 Ratio  $\langle n \rangle^{(0)} / \langle n \rangle$  as a function of  $p$ .

## References

- [1] E.V. Albano, *Heterog. Chem. Rev.* 3 (1996) 389.
- [2] V.P. Zhdanov, *Elementary Physicochemical Processes on Surfaces*, Plenum, New York (1991).
- [3] S. Rice, *Diffusion limited Reactions*, Elsevier Press, Amsterdam (1985).
- [4] Z. Rácz, *Phys. Rev. Lett.* 55 (1985) 1707.
- [5] W. Feller, *An Introduction to Probability Theory and Its Applications*, 3rd Edition, Wiley, New York, 1968.
- [6] R. Dickman in: V. Privman (Ed.), *Nonequilibrium Statistical Mechanics in One Dimension*, Cambridge University Press, Cambridge, 1997.
- [7] E.E. Fauman, R. Kopelman, *Mol. Cell. Biophys.* 6 (1989) 47.
- [8] M.E. Fisher, *J. Stat. Phys.* 53 (1988) 175.
- [9] E.W. Montroll, *J. Math. Phys.* 10 (1969) 753.
- [10] J.J. Kozak, C. Nicolis, G. Nicolis, *J. Chem. Phys.* 113 (2000) 8168.
- [11] G.H. Weiss, *J. Stat. Phys.* 15 (1976) 157.
- [12] J.B.T.M. Roerdinck, K.E. Shuler, *J. Stat. Phys.* 40 (1985) 205; *J. Stat. Phys.* 41 (1985) 581.
- [13] C. van den Broeck, *Drunks, Drift and Diffusion*, Master thesis, Vrije Universiteit Brussels, Brussels, 1988.

- [14] A. Gandjbakhche, R. Nossal, R.F. Bonner, *J. Stat. Phys.* 69 (1992) 35.
- [15] J. Noolandi, *Phys. Rev. B* 16 (1977) 4466.
- [16] G. Pfister, H. Scher, *Adv. Phys.* 27 (1978) 747.
- [17] F.W. Schmidlin, *Phys. Rev. B* 16 (1977) 2362.
- [18] O. Bénichou, B. Gaveau, M. Moreau, *Phys. Rev. E* 59 (1999) 103.
- [19] R. Elber, M. Karplus, *J. Am. Chem. Soc.* 112 (1990) 9161.
- [20] M. Tuckerman, K. Laasonen, M. Sprik, M. Parinello, *J. Chem. Phys.* 103 (1995) 150.
- [21] J. Whitmarsh and Govindjee in *Concepts in Photobiology: Photosynthesis and Photomorphogenesis*, ed. by G.S. Singhal, G. Renger, S.K. Sopory, K-D. Irrgang and Govindjee, Narosa Publishers, New Delhi and Kluwer Academic, Dordrecht (1999).
- [22] R. van Grondelle and J. Amesz in *Light Emission by Plants and Bacteria*, ed. by Govindjee, J. Amesz and D.C. Fork, Kluwer Academic, Netherlands (1986).
- [23] G.H. Weiss, *Aspects and applications of the random walk*, North-Holland, Elsevier Science B.V., Amsterdam, 1994.
- [24] J.E. Kemeny, J.L. Snell, *Finite Markov chains*, Van Nostrand, Princeton, 1960.
- [25] C.A. Walsh, J.J. Kozak, *Phys. Rev. Lett.* 47 (1982) 1500.
- [26] C. Jordan, *Calculus of finite differences*, Chelsea Pub. Comp., New York, 1979.
- [27] J.L. Bentz, J.J. Kozak, E. Abad, G. Nicolis, *Physica A* 326/1-2 (2003) 55.
- [28] D.R. Cox, H.D. Miller, *The Theory of Stochastic Processes*, Chapman and Hall, London, 1972.
- [29] C. Nicolis, J.J. Kozak, G. Nicolis, *J. Chem. Phys.* 115 (2001) 663.

## CHAPTER 4. General conclusions

### 4.1 General discussion

In this work, results, both analytic and numerical, on the role of boundary effects and of geometric factors such as size, dimensionality, and topological invariants on the efficiency of encounter-controlled reactions have been obtained. Values for the mean walklengths  $\langle n \rangle_1$  and  $\langle n \rangle_2$  for the 1WT and the 2W case as well as the relative efficiency  $\Gamma$  have been computed both for large lattices and small size systems.

The relevance of considering in detail systems of restricted spatial extent is increasing, as it is nowadays realized that heterogenous catalytic processes of great importance take place on single crystallographic faces of solid catalysts where they can involve only a few tens of particles. Despite the fact that the numerical values obtained in this work for small systems are not universal, some universal trends of a different kind have nevertheless been observed, e.g. the dependence (increasing, monotonic, etc.) of  $\Gamma$  on valency, connectivity and boundary conditions. In general, one has  $\Gamma > 1$ , implying that the reactive efficiency of two moving reactants is greater than a diffusing plus an immobile one.

Turning now to large-size systems, our results show that  $\Gamma$  increases with increasing lattice size until it reaches a well-defined limiting value  $\Gamma_\infty$ . For a given lattice geometry, this value decreases with increasing dimensionality. With the exception of the even cubic lattice,  $\Gamma_\infty > 1$ .

For Euclidean lattices of square-planar or cubic symmetry and subject to periodic boundary conditions the value of  $\Gamma_\infty^{odd}$  is exactly 2 and  $\sqrt{2}$  in one<sup>1</sup> and two dimensions respectively, and about 1.22 in three dimensions. One is tempted to advance that this last number is actually

---

<sup>1</sup>In the diffusive limit, it can be shown that the diffusion coefficient for the relative motion of both reactants is twice as large in the 2W case [30]. Discrepancies from this value for small systems are due to the discreteness of the lattice. Possibly similar arguments hold in higher dimensions.



within the precision afforded by the simulations just  $\sqrt{(3/2)}$ . Now, 1,  $\sqrt{2}$  and  $\sqrt{3}$  are the natural metrics of the lattices here considered in, respectively, 1, 2 and 3 dimensions. The results for  $\Gamma_{\infty}^{odd}$  could then be particular cases of a universal expression: the ratio of the maximum distance that two simultaneously moving reactants can traverse in one time unit before they react or find themselves in nearest neighbor positions, over the analogous quantity for the one reactant plus trap case. Further work is necessary to assert the validity of this conjecture and to understand why it manifests itself only for odd lattices.

For a given system size, the 1WT and the 2W reaction efficiency becomes less efficient when confinement is introduced, but the decrease in efficiency is smaller for the 2W case, leading to an increased value of  $\Gamma$  with respect to the periodic case. This boundary effect appears to become less significant with increasing system size, although it is not completely absent in the thermodynamic limit.

The questions raised in this work and the results obtained constitute potentially useful elements in the important problem of optimal design of the microreactors nowadays involved in chemical kinetics under nanoscale conditions. For instance, as seen in Chapter 2, a small catalytic surface in the form of a sphere or of a hexahedral surface homeomorphic to it ( $\chi = 2$ ) would enhance the reaction efficiency as compared to a surface homeomorphic to a torus ( $\chi = 0$ ). These observations highlight the need to incorporate in the design such aspects as the geometry of the microreactor, which can enhance an increasingly effective mixing of the reactants and hence an increased efficiency of the reaction itself. Finally, the role of the kinetics (linear vs. nonlinear) in modulating or enhancing the importance of such factors is certainly a problem worth addressing.

We have seen that the  $1d$  problem of computing the mean reaction time between two diffusing co-reactants can be reduced to a trapping problem for a single walker. The latter can be viewed as a generalized ruin problem, the duration of the game plays thereby the role of the mean time to absorption.

In the diffusive limit, equivalent to the limit  $N \rightarrow \infty$  if the lattice length  $L$  is held fixed, the reaction efficiency increases linearly with  $p$ , but important deviations are observed for not

too large values of  $N$ . Beyond the crossover size  $N = 4$ , a new parity effect is observed. For odd values of  $N$ , the reaction time still increases monotonically (but no longer linearly) with  $p$ , while for even values of  $N$ , the efficiency is optimized for an intermediate value  $p_{min} < 1$ . In higher dimensions, this parity effect is even more pronounced, i.e. for even lattices there is a drastic increase in efficiency when a tiny amount of synchronicity is introduced. In contrast to the  $1d$  case, the effect is enhanced with increasing  $N$ .

A generalization of results such as equation (3.23) to higher dimensional integral and fractal lattices is also of interest, since it may further clarify the role of dimensionality and the lattice coordination number. According to our results, in one-dimension two synchronously moving walkers are asymptotically twice as efficient as when they hop one after the other. In a  $2d$  square planar lattice, Kozak *et al.* have shown that the purely synchronous case is  $\sqrt{2}$  times more efficient than the purely asynchronous one in the large  $N$  limit for odd lattices [12]. The question is whether or not the relative efficiency of both processes in lattices with fractal dimension  $1 < d_f < 2$  lies between 2 and  $\sqrt{2}$ . Preliminary calculations on a Sierpinski gasket (with fractal dimension  $d_f = 1.585$ ) seem to indicate an asymptotic relative efficiency higher than 2 in this case, despite the fact that the lattice has (up to the three vertex sites) the same coordination number as a  $2d$  square planar lattice [31]. The reason for this may be the important role played by the specific form of the lattice boundaries, even in the limit of a large lattice. This may motivate the study of boundary conditions other than periodic ones for the two-walker system. However, the analytical treatment of this case is considerably harder, at least in the framework of the method of difference equations, since the lattice is no longer translationally invariant.

## 4.2 Future research

As a further extension of our work, one can also consider more complex reactive schemes [32] involving more than two walkers to study the combined effect of synchronicity and many-body effects. Other avenues for further research concern revisiting the 1WT and 2W reaction schemes and adding further conditions to the transitions of the reactants. In the work presented thus

far, the transition probabilities were dependent only on the geometry of the lattice and number of nearest neighbor sites.<sup>2</sup> One could apply some electrostatic potential to the reactants which would allow the study of long-range interactions. One can also consider more complicated reaction schemes which involve more than two reactants and which may have more than one reaction pathway. For example, one could formulate the geometry in such a way as to have immobile catalyst sites as well as mobile reactants. This study has already begun and some preliminary results have been reported [32].

---

<sup>2</sup>In the synchronous vs. asynchronous work there was a non-zero probability for a reactant to remain stationary at a particular time step, but when the reactant did finally make a jump, the transition probability was still defined exclusively by the number of allowable nearest neighbor sites available.

## APPENDIX One Dimensional Example

Consider a  $1d$  lattice with periodic boundary conditions. The problem of the random walker and a single trap can be solved for an exact expression at least three different ways. Montroll solved the problem through the use of generating functions [11]. Two other methods will be outlined in more detail below and can also be seen in ref. [33].

### Difference equation method

One method is through the use of difference equations. Recall that the expression to solve is

$$\langle n \rangle \equiv \frac{1}{N-1} \sum_{z=1}^{N-1} \langle n \rangle_z, \quad (\text{A.1})$$

where the factor of  $N-1$  in the denominator is present to avoid over-counting the lattice sites since site  $N$  is the trap, and  $z$  denotes the index of the lattice site. The difference equation one must solve is the following,

$$\langle n \rangle_z = \frac{1}{2} \langle n \rangle_{z+1} + \frac{1}{2} \langle n \rangle_{z-1} + 1, \quad 0 < z < N, \quad \langle n \rangle_0 = \langle n \rangle_N = 0, \quad (\text{A.2})$$

where the addition of unity is included because the walklength should be incremented by 1 with each time step. Multiplication by the constant factor 2 and rearrangement puts the equation in a more useful form

$$\langle n \rangle_{z+1} - 2\langle n \rangle_z + \langle n \rangle_{z-1} = -2. \quad (\text{A.3})$$

The theory of inhomogeneous, second-order linear difference equations with constant coefficients specifies that the solution will be composed of the solution to the homogeneous difference equation and the particular solution [34]. Upon inspection, the characteristic equation is

$$m^2 - 2m + 1 = 0, \quad (\text{A.4})$$

which has a double root at  $m = 1$ . Since there is a double root, the solution to the homogeneous equation has the form

$$\langle z \rangle_z^{\text{hom.}} = C_1 m^z + C_2 z m^z \quad (\text{A.5})$$

and since the double root is 1 the expression is

$$\langle z \rangle_z^{\text{hom.}} = C_1 + C_2 z. \quad (\text{A.6})$$

If the inhomogeneous term is of the form  $A(b)^z$ , then the particular solution will be of the form  $A_0(b)^z$ . Since the inhomogeneous term in this case is  $-2(1)^z$ , the particular solution should be  $A_0(1)^z$ . But since  $(1)^z$  and  $z(1)^z$  are already part of the solution to the homogeneous equation, the correct particular solution is  $A_0 z^2 (1)^z$ . To determine  $A_0$ , we substitute the particular solution into Eq. (A.3) for  $\langle n \rangle_z$  which yields

$$A_0(z+1)^2 - 2A_0 z^2 + A_0(z-1)^2 = -2. \quad (\text{A.7})$$

After performing the algebra and some cancellations, one finds that  $A_0 = -1$ . The full solution is now

$$\langle n \rangle_z = C_1 + C_2 z - z^2. \quad (\text{A.8})$$

To determine the constants it is necessary to utilize the boundary conditions with Eq. (A.8).

This becomes the two-equation system

$$\langle n \rangle_0 = 0 = C_1 \quad (\text{A.9})$$

$$\langle n \rangle_N = 0 = C_1 + C_2 N - N^2. \quad (\text{A.10})$$

Upon evaluation of the constants, the full expression is

$$\langle n \rangle_z = z(N - z). \quad (\text{A.11})$$

Now substituting Eq. (A.11) into Eq. (A.1) yields

$$\langle n \rangle = \frac{1}{N-1} \sum_{z=1}^{N-1} z(N-z), \quad (\text{A.12})$$

where the summation is evaluated analytically as

$$\sum_{z=1}^{N-1} z(N-z) = \frac{N(N+1)(N-1)}{6}. \quad (\text{A.13})$$

Performing the division by  $N - 1$  finally gives the expression for the mean walklength

$$\langle n \rangle = \frac{N(N+1)}{6}. \quad (\text{A.14})$$

### Markov transition matrix method

Another method used to solve the mean walklength problem is through the so-called Markov method [27, 29]. This involves constructing a probability matrix and inverting the matrix to yield all the individual walklengths from each symmetry distinct site, and then summing them up to form the overall walklength. Consider as an example Fig. A.1, a 5-site 1d chain with

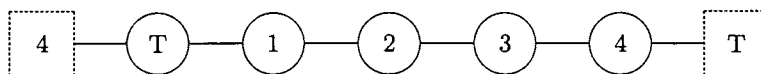


Figure A.1 One dimensional 5-site lattice, with the sites in the circles denoting the lattice sites and the dashed boxes denoting the connectivity of the terminal sites due to the periodicity of the lattice.

periodic boundary conditions and a deep trap. With this figure in mind one constructs the probability matrix  $\mathbf{P}$  which describes all the probabilities of movement for a random walker. Each element  $P_{ij}$  describes the probability of a walker on site  $i$  moving to site  $j$  in the next time step. The probability matrix in this case is

$$\mathbf{P} = \begin{bmatrix} 1 & 0 & 0 & 0 & 0 \\ 1/2 & 0 & 1/2 & 0 & 0 \\ 0 & 1/2 & 0 & 1/2 & 0 \\ 0 & 0 & 1/2 & 0 & 1/2 \\ 1/2 & 0 & 0 & 1/2 & 0 \end{bmatrix}. \quad (\text{A.15})$$

$\mathbf{P}$  can be decomposed into 4 blocks as

$$\mathbf{P} = \begin{bmatrix} \mathbf{L} & \mathbf{0} \\ \mathbf{R} & \mathbf{Q} \end{bmatrix}. \quad (\text{A.16})$$

In this decomposition,  $\mathbf{L}$  describes the ergodic or equilibrium state,  $\mathbf{R}$  describes the transitions from the transient states to the ergodic states, and  $\mathbf{Q}$  describes all the transitions between

transient states. The appropriate partitioning of  $\mathbf{P}$  is

$$\mathbf{L} = [1], \quad \mathbf{R} = \begin{bmatrix} 1/2 \\ 0 \\ 0 \\ 1/2 \end{bmatrix}, \quad \mathbf{0} = \begin{bmatrix} 0 & 0 & 0 & 0 \end{bmatrix}, \quad (\text{A.17})$$

and

$$\mathbf{Q} = \begin{bmatrix} 0 & 1/2 & 0 & 0 \\ 1/2 & 0 & 1/2 & 0 \\ 0 & 1/2 & 0 & 1/2 \\ 0 & 0 & 1/2 & 0 \end{bmatrix}. \quad (\text{A.18})$$

Once  $\mathbf{Q}$  is specified, the theory of Markov chains shows that matrix  $\mathbf{N} = (\mathbf{I} - \mathbf{Q})^{-1}$  (called the fundamental matrix) can be computed and from it the walklength data can be extracted. In this particular example  $\mathbf{N}$  is

$$\mathbf{N} = \begin{bmatrix} 8/5 & 6/5 & 4/5 & 2/5 \\ 6/5 & 12/5 & 8/5 & 4/5 \\ 4/5 & 8/5 & 12/5 & 6/5 \\ 2/5 & 4/5 & 6/5 & 8/5 \end{bmatrix}. \quad (\text{A.19})$$

The elements  $N_{ij}$  denote average site visitation values, that is, for a walker starting at site  $i$ , it will visit site  $j$  an average of  $N_{ij}$  times before being trapped irreversibly. This leads to the fact that the sum of any particular row  $i$  of the matrix  $\mathbf{N}$  gives the average lifetime of a walker starting from site  $i$  and ultimately terminating the walk at the trap. Formally speaking this is expressed as

$$\langle n \rangle_z = \sum_j N_{zj}. \quad (\text{A.20})$$

In this particular example we have

$$\langle n \rangle_1 = 4, \quad \langle n \rangle_2 = 6, \quad \langle n \rangle_3 = 6, \quad \langle n \rangle_4 = 4, \quad (\text{A.21})$$

for the walklengths from each individual site and

$$\langle n \rangle = \frac{1}{4} \{ \langle n \rangle_1 + \langle n \rangle_2 + \langle n \rangle_3 + \langle n \rangle_4 \} = 5, \quad (\text{A.22})$$

for the overall average walklength. This result is corroborated with the result which is calculated using Eq. (A.14) when  $N = 5$ .<sup>3</sup> Recall from Chapter 1.1 that the inverse of the smallest eigenvalue of  $\mathbf{G}$  is related to the mean walklength as well [Eq. (1.10)]. This provides an independent check on our results. In our context here,  $\mathbf{G}$  is given by

$$\mathbf{G} = \mathbf{I} - \mathbf{Q} = \begin{bmatrix} 1 & -1/2 & 0 & 0 \\ -1/2 & 1 & -1/2 & 0 \\ 0 & -1/2 & 1 & -1/2 \\ 0 & 0 & -1/2 & 1 \end{bmatrix}. \quad (\text{A.23})$$

The eigenvalues of  $\mathbf{G}$  are

$$\lambda_1 = \frac{3}{4} - \frac{1}{4}5^{1/2} \quad (\text{A.24})$$

$$\lambda_2 = \frac{3}{4} + \frac{1}{4}5^{1/2} \quad (\text{A.25})$$

$$\lambda_3 = \frac{5}{4} - \frac{1}{4}5^{1/2} \quad (\text{A.26})$$

$$\lambda_4 = \frac{5}{4} + \frac{1}{4}5^{1/2} \quad (\text{A.27})$$

and  $\lambda_1^{-1} \simeq 5.236$ , which agrees quite nicely with our earlier result of 5 which we already obtained from both methods.

Notice that this particular solution of the Markov transition matrix does not give a general solution as does the method of generating functions and the method of difference equations. It only gives a particular solution to a case on a finite lattice with well-defined walker and boundary conditions. The general solution can be determined by recognizing patterns in the mean walklength values of the first few small lattices.

The power of the Markov transition matrix method is apparent when dealing with dimensions higher than 1. Constructing the transition matrix in higher dimensions and solving for the site-individual and overall mean walklengths poses no new theoretical or mathematical problems. While exact analytic solutions may not be possible in higher dimensions, the numerical results provided by Markov theory still yield a great deal of information about the particular system in question. The methods of difference equations and generating functions

---

<sup>3</sup>In this example case there are 5 sites on the lattice. There are 4 transient sites and 1 deep trap.



are not easily solved in dimensions higher than 1 and for that reason they provide elegant solutions in  $1d$  but in higher dimensions are not as helpful.

## REFERENCES

- [1] A.V. Barzykin, K. Seki, M. Tachiya, *Adv. Coll. Inter. Sci.* 89-90 (2001) 47.
- [2] E.V. Albano, *Heterog. Chem. Rev.* 3 (1996) 389.
- [3] V.P. Zhdanov, *Elementary Physicochemical Processes on Surfaces*, Plenum, New York (1991).
- [4] N. Pavlenko, J.W. Evans, D.-J. Liu, R. Imbihl, *Phys. Rev. E* 65 (2001) 016121.
- [5] S. Rice, *Diffusion Limited Reactions*, Elsevier Press, Amsterdam (1985).
- [6] Z. Rácz, *Phys. Rev. Lett.* 55 (1985) 1707.
- [7] W. Feller, *An Introduction to Probability Theory and Its Applications*, 3rd Edition, Wiley, New York, 1968.
- [8] R. Dickman in: V. Privman (Ed.), *Nonequilibrium Statistical Mechanics in One Dimension*, Cambridge University Press, Cambridge, 1997.
- [9] E.E. Fauman, R. Kopelman, *Mol. Cell. Biophys.* 6 (1989) 47.
- [10] M.E. Fisher, *J. Stat. Phys.* 53 (1988) 175.
- [11] E.W. Montroll, *J. Math. Phys.* 10 (1969) 753.
- [12] J.J. Kozak, C. Nicolis, G. Nicolis, *J. Chem. Phys.* 113 (2000) 8168.
- [13] G.H. Weiss, *J. Stat. Phys.* 15 (1976) 157.
- [14] J.B.T.M. Roerdinck, K.E. Shuler, *J. Stat. Phys.* 40 (1985) 205; *J. Stat. Phys.* 41 (1985) 581.

- [15] C. van den Broeck, Drunks, Drift and Diffusion, Master thesis, Vrije Universiteit Brussels, Brussels, 1988.
- [16] A. Gandjbakhche, R. Nossal, R.F. Bonner, *J. Stat. Phys.* 69 (1992) 35.
- [17] J. Noolandi, *Phys. Rev. B* 16 (1977) 4466.
- [18] G. Pfister, H. Scher, *Adv. Phys.* 27 (1978) 747.
- [19] F.W. Schmidlin, *Phys. Rev. B* 16 (1977) 2362.
- [20] O. Bénichou, B. Gaveau, M. Moreau, *Phys. Rev. E* 59 (1999) 103.
- [21] R. Elber, M. Karplus, *J. Am. Chem. Soc.* 112 (1990) 9161.
- [22] M. Tuckerman, K. Laasonen, M. Sprik, M. Parinello, *J. Chem. Phys.* 103 (1995) 150.
- [23] J. Whitmarsh and Govindjee in *Concepts in Photobiology: Photosynthesis and Photomorphogenesis*, ed. by G.S. Singhal, G. Renger, S.K. Sopory, K-D. Irrgang and Govindjee, Narosa Publishers, New Delhi and Kluwer Academic, Dordrecht, 1999.
- [24] R. van Grondelle and J. Amesz in *Light Emission by Plants and Bacteria*, ed. by Govindjee, J. Amesz and D.C. Fork, Kluwer Academic, Netherlands, 1986.
- [25] N.G. van Kampen, *Stochastic Processes in Physics and Chemistry*, North-Holland, Elsevier Science Publishers B.V., Amsterdam, 1992.
- [26] G. Nicolis, I. Prigogine, *Self-Organization in Nonequilibrium Systems*, John Wiley & Sons, New York, 1977.
- [27] J.J. Kozak, *Adv. Chem. Phys.* 115 (2000) 245.
- [28] G.H. Weiss, *Aspects and applications of the random walk*, North-Holland, Elsevier Science B.V., Amsterdam, 1994.

- [29] J.G. Kemeny, J.L. Snell, Finite Markov chains, Springer-Verlag, New York, 1976.
- [30] E. Abad, G. Nicolis, J.L. Bentz, J.J. Kozak, Physica A 326/1-2 (2003) 69.
- [31] J.L. Bentz, J.J. Kozak, E. Abad, G. Nicolis, Physica A 326/1-2 (2003) 55.
- [32] C. Nicolis, J.J. Kozak, G. Nicolis, J. Chem. Phys. 115 (2001) 663.
- [33] E. Abad, Aspects of Nonlinear Dynamics in Low Dimensional Lattices: a Multilevel Approach, PhD Thesis, Université Libre de Bruxelles, Brussels, 2003.
- [34] S. Goldberg, Introduction to Difference Equations, John Wiley & Sons, Inc., New York, 1958.

## ACKNOWLEDGEMENTS

I would like to take this opportunity to express my thanks to those who helped me with various aspects of conducting research and the writing of this thesis. First and foremost, Dr. John J. Kozak for his guidance, patience, and support throughout this research and the writing of this thesis. I would also like to thank my committee members for their efforts and contributions to this work: Dr. Jim Evans, Dr. Xueyu Song, Dr. Gerald Small, and Dr. Mark Gordon.

I would like to thank Dr. Gregoire Nicolis for his kindness and unique insights in our work together. Thanks are also in order to Dr. Enrique Abad (who just received his PhD), my principal graduate student collaborator, for his time and willingness to be a teacher to me. Thank you as well to another fellow graduate student collaborator Fatemeh Niroomand Hosseini, who performed some very tedious calculations in our work together.

I would like to thank the Department of Chemistry office staff for helping me fill out the proper paperwork and meet all the deadlines.

Lastly, I thank my family for their support, and a special thanks to my wife Jennifer, who has supported me throughout my graduate education and because of her unselfishness, has allowed me to pursue my academic and personal goals vigorously.